Earth Science Informatics (2024) 17:4473–4505
https://doi.org/10.1007/s12145-024-01401-8

RESEARCH

Comparative analysis of SPI, SPEI, and RDI indices for assessing spatio-temporal variation of drought in Türkiye

Fatma Yaman Öz[1] · **Emre Özelkan**[2] · **Hasan Tatlı**[3]

Received: 9 April 2024 / Accepted: 26 June 2024 / Published online: 8 July 2024

Abstract

This research presents a comprehensive drought analysis using climate data obtained from 219 homogeneously distributed meteorological stations in Türkiye between 1991 and 2022. In this context, Standard Precipitation Index (SPI), Standardized Precipitation Evapotranspiration Index (SPEI) and Reconnaissance Drought Index (RDI) drought indices were used and comparative analysis was made. Türkiye. The study demonstrates that below-normal precipitation over extended periods and increasing temperatures have contributed to the increased frequency of meteorological drought events. Türkiye's topographic conditions, particularly its location in the Mediterranean basin, significantly influence drought occurrences. It is noted that over the past 20 years, Türkiye has been trending towards drier conditions, with rising temperatures reinforcing this trend. The study observes that the moderate drought class range is the most frequently recurring in the SPI, SPEI, and RDI methods utilized. Regarding atmospheric conditions affecting the climate in Türkiye, it is observed that increased drought severity stands out prominently in years when the North Atlantic Oscillation is positive. During these years, increased drought severity is evident in the SPI, SPEI, and RDI indices, particularly in winter and autumn, while a wide area experiences drought effects in the summer months. Long-term analyses emphasize that drought periods occur less frequently but have more prolonged impacts, attributed to variations in precipitation patterns from year to year and the influence of rising temperatures due to global climate change. The potential future increase in drought in the Mediterranean basin due to global climate change and Türkiye's vulnerability to this situation could have adverse effects on water resources, food security, energy sources, and ecosystems.

Keywords SPI · SPEI · RDI · Drought

Introduction

Since the mid-twentieth century, the increasing impact of anthropogenic global climate change has brought about a rise in the frequency, intensity, and impact of extreme meteorological events, with drought undoubtedly being the most devastating when considering its long-term effects (Olsen et al. 2023).

Drought is a water deficit situation that occurs when natural water resources, utilized by various systems, fall below the long-term average or normal for a specific period and at a regional scale (Türkes 2007). Due to reduced precipitation and increasing temperatures, drought extending over one or more seasons and even spanning years is a meteorological disaster. Among the natural disasters worldwide, 28 out of 31 are meteorologically-related, with drought being the most hazardous (Partigöc and Sogancı 2019). Drought possesses the characteristic of affecting larger populations

Communicated by: H. Babaie

✉ Fatma Yaman Öz
fatmayamanoz.comu@gmail.com

[1] Department of Geography, Faculty of Humanities and Social Sciences, Çanakkale Onsekiz Mart University, 1720 Çanakkale, Türkiye

[2] Department of City and Regional Planning, Faculty of Architecture and Design and Risk Management of Natural Disasters Program, School of Graduate Studies, Remote Sensing Research and Application Center, Çanakkale Onsekiz Mart University, 1720 Çanakkale, Türkiye

[3] Department of Geography, Physical Geography Division, Climatology/Meteorology, Faculty of Humanities and Social Sciences, Çanakkale Onsekiz Mart University, 1720 Çanakkale, Türkiye

negatively compared to other disasters, owing to its slow onset and extensive coverage. Beginning with precipitation deficiency, drought encompasses a four-stage process (Mishra and Singh 2010) The first stage is meteorological drought, where precipitation falls below normal levels (Wilhite and Glantz 1985; Mishra and Singh 2010). The second stage is agricultural drought, when there is not enough water to meet the needs of crops and occurs after moisture loss and scarcity in water resources (Wilhite and Glantz 1985; Dai et al. 2020; Guo et al. 2020) The third stage is hydrological drought, where a prolonged lack of rainfall causes a reduction in water resources (Wilhite and Glantz 1985; Guo et al. 2020). The final stage is socio-economic drought, which encompasses the impact of drought on agriculture, living organisms, water resources, and sectors reliant on these resources, as well as the inability to meet water demand as an economic input, negatively affecting overall societal well-being in terms of quality of life, health, employment, and livability (Mishra and Singh 2010; Moriondo et al. 2011; Rousta et al. 2023).

The socio-economic impacts of drought, closely associated with various fields such as ecosystems, agriculture, and livestock, often lead to significant problems. Furthermore, the extensive and prolonged influence of drought on large areas increases the importance of management and adaptation efforts compared to other meteorological disasters (Sahana and Mondal 2023) Therefore, studies examining the effects of drought and regional drought analyses hold a significant share in the literature, prioritizing academic language and commonly used geographical terms (Mishra and Singh 2010; Ali et al. 2011; Sobral et al. 2018; Tigkas et al. 2019; Lim Kam Sian et al. 2023). For this reason, many drought indices have been developed to determine the temporal and spatial changes of meteorological drought in the world and in our country. Drought indices can be divided into two types: parametric indices and non-parametric indices. While parametric drought indices consider a certain statistical distribution based on long-term data sets in drought assessments, non-parametric drought indices are based on calculations that are independent of the data distribution (Soľáková et al. 2013). As parametric methods are based on statistical theory, they are more reliable and allow comparisons to be made between different geographical regions. This is why they are the preferred method in the literature (Soľáková et al. 2013). The main parametric indices are Standardised Precipitation Index (SPI) (McKee et al. 1993), Standardized Precipitation Evapotranspiration Index (SPEI) (Vicente-Serrano et al. 2010) Palmer Drought Severity Index (PDSI) (Palmer 1965), De Martonne Drought Index (DAI) (De Martonne 1926), non-parametric drought indices are Reconnaissance Drought Index (RDI) (Tsakiris et al. 2007), Effective Drought Index (EDI) (Byun and Wilhite 1999) and Percentage of Normal Index (PNI) (Willeke et al. 1994) (Zargar et al. 2011; Zarei et al. 2021; Ndayiragije and Li 2022).

In this study, the most preferred indices for investigating meteorological drought are SPI, SPEI, and RDI. Among these indices, the Standardized Precipitation Index (SPI) is particularly favored due to its ease of calculation using only precipitation data, comparability across different climatic conditions, and facilitation of representing wet/dry periods (WMO 2012; Ndayiragije and Li 2022). However, the SPI method's focus on temporal changes in precipitation can overlook variations in other climatic variables (Ndayiragije and Li 2022; Kapluhan 2023; Pekpostalcı et al. 2023). Numerous studies worldwide have utilized SPI to examine wet/dry periods, contributing to the generation of insights into future drought development (Das et al. 2020; Malik and Kumar 2021; Isia et al. 2023; Miro et al. 2023; Yang et al. 2023). Another drought index preferred in the study is the Standardized Precipitation Evapotranspiration Index (SPEI), which is calculated similarly to the SPI formula. However, unlike SPI, SPEI takes into account both precipitation and evapotranspiration (ET). ET, reflecting the impact of the relationship between temperature and evaporation on drought, (Mehr et al. 2020), makes SPEI a more sophisticated method compared to SPI. In various studies in the literature, SPI, SPEI, and RDI indices have been compared to determine meteorological drought in different climatic regions and assess its impact on agricultural production (Xu et al. 2015; Pathak and Dodamani 2020; Zarei et al. 2021). Similar to the SPEI index, another preferred index used in the study is the Reconnaissance Drought Index (RDI), which incorporates both precipitation and ET (Jabbi et al. 2021). The RDI and SPEI indices provide similar climatic information. However, while RDI adopts a more general approach to rainfall distribution and assessment, SPEI is advantageous for determining agricultural drought and evaluating the impact of the temperature-evaporation relationship on drought (Tsakiris et al. 2007; Sobral et al. 2018; Zarei et al. 2021; Abbes et al. 2023). The similarity in the climatic parameters used to calculate SPI, RDI, and SPEI indices enables comparisons, and their utilization in the study is favored due to their ability to depict spatial variations and similarities in describing them.

In studies utilizing drought indices to analyze the spatial–temporal variation of drought, interpolation methods developed to generate data in locations without data are commonly used. Stochastic methods such as Kriging, which consider spatial autocorrelation, have been successfully used in analyzing the spatial and temporal distribution of drought (Moreira et al. 2008; Akhtari et al. 2009; Gocic and Trajkovic 2013). For Türkiye, which has a wide and varied geography, studies involving the interpolation of climatological data have determined that Ordinary Kriging is the method that best represents spatial

distribution (Yavuz and Erdoğan 2012; Aydın, 2014; Ozelkan et al. 2015; Cağlıyan and Ayhan 2018; Khorrami and Gündüz 2021). In our study, the Ordinary Kriging method was chosen for the spatial interpolation of drought data. The implementation of drought methods and the creation of maps were conducted in a Geographic Information Systems (GIS) environment.

The Mediterranean basin is referred to as a 'hotspot of climate change' according to climate models (Lionella and Scarascia 2018; Lange 2020). Due to its location in a dry and semi-drought climate region and the combination of increasing temperatures with decreasing rainfall, it is anticipated that the impact of climate change will intensify, leading to more severe droughts in the Mediterranean basin (Türkes 2020a; Erlat and Güler 2023). Particularly in the Mediterranean basin, an increase in annual temperatures by 25% above the global average and 40% more during summer months is expected by the mid to late twenty-first century (Lionella and Scarascia 2018). This situation contributes to an increased vulnerability of Türkiye to drought events and other potential impacts of global climate change. Therefore, rising temperatures and decreasing precipitation values may lead to adverse effects on factors such as water resources, food security, energy sources, terrestrial and marine ecosystems, and human health and safety. In recent times, the direct impact of drought on water resources and water management, especially in extensive geographic areas with pronounced effects of climate change such as Türkiye with its dry and semi-drought climate characteristics, is among the most intensively researched topics. The severity of drought in Türkiye and its accurate prediction are of vital importance for the sustainable management of water resources. The effects of climate change have been increasing recently. Therefore, climate change and the reasons for it and situations causing serious problems such as drought need to be updated. Previous studies have looked at specific drought years and specific areas. This study covers the current data of the last few years and at the same time constitutes a whole of the studies carried out in the past periods. For this reason, the aim of this study is to reveal the temporal and spatial changes of drought in Türkiye using different drought indices and to evaluate the impact of drought on atmospheric circulation systems with current data. In this context, the main objectives of this study are as follows:

- Between 1991 and 2022, the comparison of the severity of drought in Türkiye using SPI/SPEI and RDI indices for 1, 3, 6, 9, and 12-month periods across stations in the study area, and determination of the driest/moistest years by month,
- Determination and comparison of average frequency values of drought classes over years for SPI/SPEI and RDI methods between 1991 and 2022,
- Spatial distribution of the driest years identified for each index type will be mapped using Geographic Information Systems (GIS) to depict changes in drought severity in Türkiye for those years.

The subsequent sections will describe the general characteristics of the study area, the meteorological data used, and the methods employed in processing this data and analyzing the temporal and spatial changes in drought.

Data and methods

This section will sequentially describe the general characteristics of the study area, the meteorological data used, and the processing of this data, as well as the methods employed in analyzing the temporal and spatial changes in drought. In the study, drought indices of SPI, SPEI, and RDI for 1, 3, 6, 9, and 12-month periods were calculated for 219 stations between 1991 and 2022. These calculations were examined in four stages:

1. Average frequency values for each year were generated based on drought classes to compare which drought class occurred most frequently in each year according to the drought indices.
2. The driest and wettest years for each month between 1991 and 2022 were determined in all drought indices, along with the corresponding regions where these values were observed in the study area.
3. The driest years for each month were identified in each drought method, and spatial distribution maps were created for these years.
4. The results of the conducted studies were evaluated.

The data and methods to be used within this scope are explained as follows:

Study area

The study area covers an area of 783,562 km^2 between 36°-42° North latitude and 26°-45° East longitude (Fig. 1). The average elevation is 1132 m and the region is located in the Mediterranean major climatic zone of the Subtropical belt. However, the diversity of landforms and especially the presence of mountains running parallel to the coast cause climatic conditions to vary from region to region. While the coastal areas have milder climatic conditions, the inland parts of the Anatolian plateau are characterized by hot summers, cold winters and low rainfall. According to the Thornthwaite climate classification, arid regions are in the interior, east and southeast of the study area (Fig. 2) (Sensoy et al. 2008). Humid regions are located in the northern

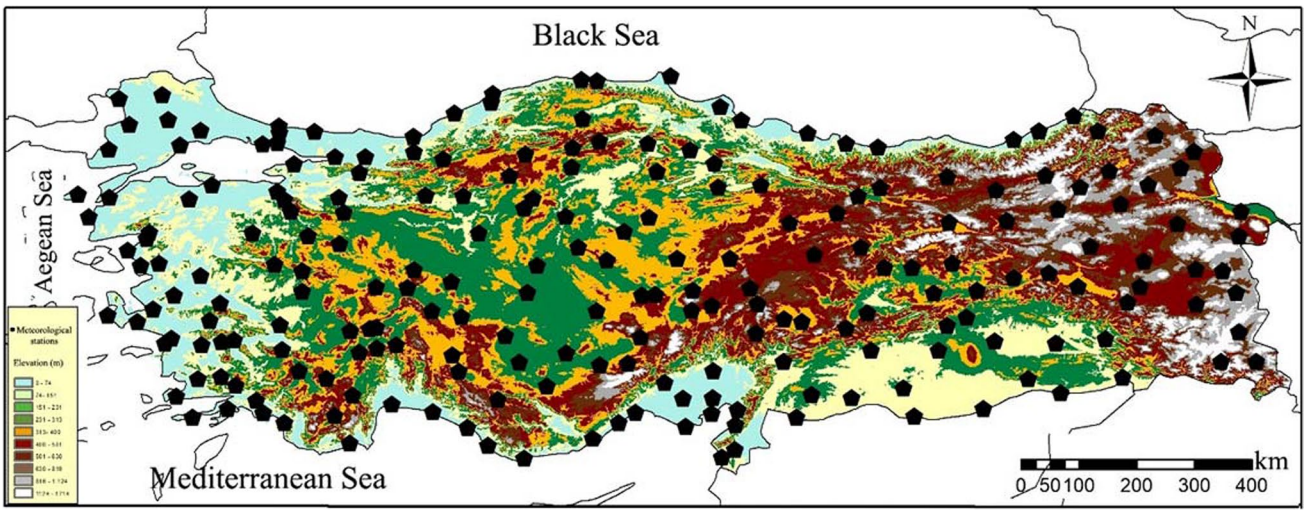

Fig. 1 Meteorological stations in the study area

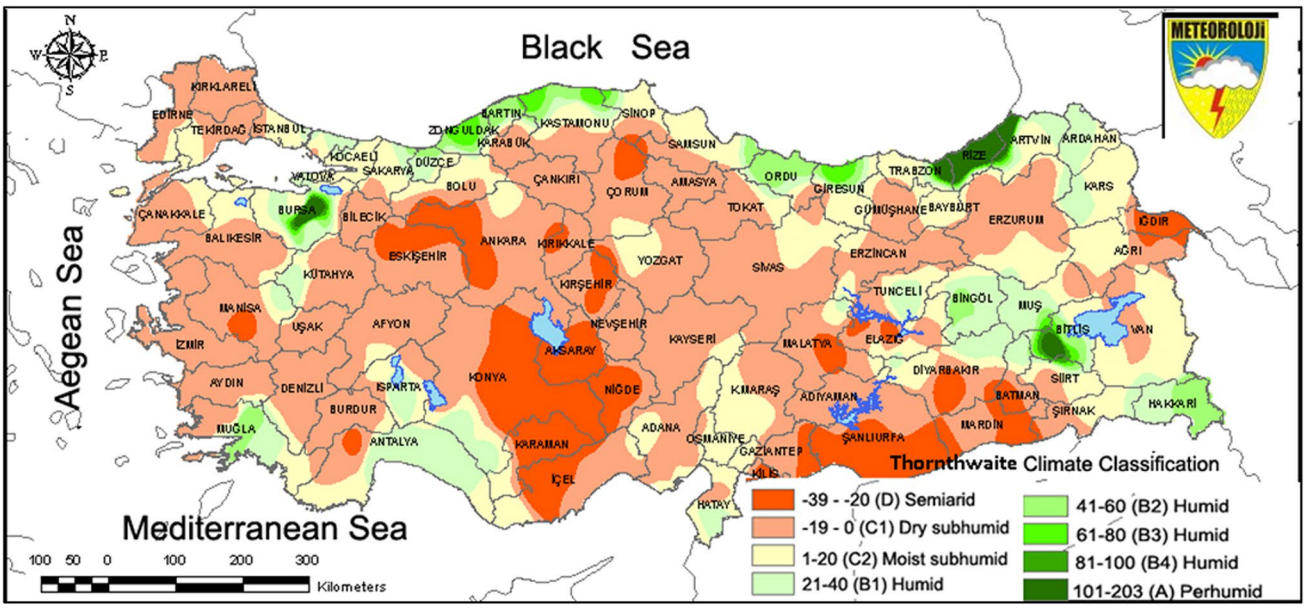

Fig. 2 Climate classification of Türkiye according to Thorntwaite precipitation index (Sensoy et al. 2008)

parts, around Bitlis city (located in the south of Türkiye) and in the southwest (Fig. 2). The other regions of Turkey are generally characterised by semi-arid and semi-humid climate zones. The Mediterranean climate zone, where Turkey is located, is highly affected by global climate change due to being under the influence of mobile mid-latitude and Mediterranean depressions (Olgen 2010). The frequency and effectiveness of mobile depressions, high atmospheric pressure, westerly winds and polar jet stream caused by the Mediterranean front and the Polar front control the precipitation conditions, which causes the occurrence of dry periods (Kömüscü, 2001). Apart from the effect of depressions due to its location, precipitation regimes and variability in Türkiye are also affected by atmospheric controls such as the North Atlantic Oscillation (NAO). In particular, periods with positive NAO anomalies correspond to dry periods over Türkiye (Kömüscü, 2001). At the same time, the fact that Türkiye is surrounded by seas on three sides, the increase in the average elevation from west to east and the direction of extension of the mountains cause differentiation of climate characteristics in short distances (Sensoy et al. 2008). These geographical features of Türkiye bring about spatial and temporal variations in precipitation and temperature due to atmospheric controls and microclimatic

zones. This change also causes regional rainfall irregularity, water shortage and drought effects. While the areal precipitation value for 2022 is 503.8 mm in Türkiye, the average areal precipitation between 1991 and 2020 is 573.4 mm. The average temperature value is 13.9 °C (MGM 2022). According to the 2022 climate assessment report, the highest temperature was 47.9 °C in July in Şırnak/Silopi and the lowest temperature was -34.4 °C in January in Van/Özalp (MGM 2023). According to 2022 data, the highest precipitation was 87 mm in January and the lowest precipitation was 9 mm in July (MGM 2023). Climatic differences in the study area cause changes in the natural vegetation cover in a short distance, forming various formations such as forest, shrubs and grasses (Avcı, 2005; Günal 2013).

Meteorological data

Monthly total precipitation data and monthly maximum, minimum and average maximum, minimum and average temperature data measured between 1991 and 2022 at 219 meteorological observation stations across Türkiye (Fig. 1) belonging to the General Directorate of Meteorology of the Ministry of Environment, Urbanization and Climate Change of the Republic of Türkiye were used to calculate the SPI, RDI and SPEI drought indices. The main reason for selecting this period is the lack of missing data in the measurements made for all stations during the observation period between 1991 and 2022.

Determination of average frequency values

Seven drought classes used in the evaluation of drought indices were determined. The recurrence rates of these drought classes for each year were determined and graphs were created according to their average values. As a result, interpretations were made according to the change in the average recurrence values of the drought classes in which year.

Drought indices

Standard precipitation index

SPI is considered as a statistically correlated index calculated based on the probability of precipitation in a given time period (Mlenga et al. 2019) (1). The first period when the index falls below zero is considered the beginning of drought, and the month when the index rises to a positive value is considered the end of drought (McKee et al. 1993). In the classical approach of SPI, the cumulative distribution function of rainfall totals is fitted to the appropriate frequency distribution (McKee et al. 1993). In SPI, precipitation is converted into normalized common units based on numerical measurements (Türkeş and Tatlı, 2009; Badji et al. 2023). The number of standard deviations refers to the deviation of standard measurements from the long-term average (Mlenga et al. 2019). As a result, SPI can be used for normal, log-normal and gamma distributions of precipitation (Zeybekoglu et al. 2023). In this study, drought analyses were calculated with the R-Studio package program and it is assumed that the intensity function of precipitation in a given period fits the following gamma distribution (1):

$$g(x) = \frac{1}{\beta^{\alpha}\Gamma(\alpha)} x^{a-1} e^{-x/\beta} x > 0 \quad (1)$$

The continuation of the formulas given in accordance with the Gaussian distribution can be found in the sources. In this section, only the first and the last part of the formula are given (see e.g. following references for a similar approach: (Lim Kam Sian et al. 2023). SPI is the average of the difference of the precipitation total for a studied time period from the long-term average for that time period, again obtained from the long-term data for that time period.

$$SPI = \frac{\left(X_i - X_{ort}\right)}{\sigma} \quad (2)$$

where X_i represents the precipitation total within the time period, $\overline{X}$ represents the long-term average of the precipitation totals within the studied time period, and σ represents the long-term standard deviation of the relevant time period (2) (Tatlı et al. 2004; Tatlı and Türkes 2008; Ozelkan and Karaman 2018). The obtained SPI values can be calculated for different periods (such as 1, 3, 6, 9, 12, 24, 48 months) and these values can be subjected to the classification given in Table 1.

Standardized precipitation evapotranspiration index

SPEI is used to assess the severity of agricultural drought, taking into account plant evapotranspiration and meteorological drought. SPI is calculation-based and expressed as the difference (D) between potential evapotranspiration (PET) and precipitation (P) (3). This difference (D) constitutes

Table 1 Drought analysis classification values (Zarei et al. 2021)

SPI, SPEI or RDI	Moisture Categories
≥2.0	Extremely Wet
1.5 to 1.99	Severe wet
1.0 to 1.49	Moderately wet
0.99 to -0.99	Normal
-1.00 to -1.49	Moderately Drought
-1.50 to -1.99	Severe Drought
≤-2.00	Extremely drought

the water surplus or deficit for the analyzed month (i) (Bakanogulları 2020; Badji et al. 2023).

$$D_i = P_i - PET_i \tag{3}$$

In SPEI calculation, unlike SPI analysis, the difference between precipitation and PET (D) is calculated as water deficit. After the accumulated precipitation is converted into probabilities, these probabilities are transformed into a standard distribution to form drought index values. In this way, SPEI values represent the number of standard deviations from total precipitation or climatic water deficit for a given location and year (Stagge et al. 2015). The classification of the value ranges used for the evaluation of the analyses is shown in Table 1.

Reconnaissance drought index

RDI (Reconnaissance Drought Index), which is one of the most widely used indices in drought analysis, is advantageous for calculating PET like SPEI. Indices such as SPI and SPEI are calculated based on precipitation and temperature factors and are important in evaluating PET values and agricultural productivity (Tsakiris et al. 2007). The RDI was presented at the MEDROPLAN coordination meeting as a new drought analysis method and has been described in more detail in other publications (Tsakiris 2004; Tsakiris and Vangelis 2005).

A detailed calculation of the formula can be found in the references. The last step of the formula is given in this section (see e.g. following references for a similar approach: (Tsakiris and Vangelis 2005; Tsakiris et al. 2007; Zarei et al. 2021).

$$RDI_{st} = \frac{\sum_{i=1}^{N}\left(a_0^{(i)} - \overline{a_0}\right)}{\sqrt{\frac{1}{N}\sum_{i=1}^{N}(a_0^{(i)} - \overline{a_0})^2}} \tag{4}$$

In this formula, RDI_{st} represents the standardized RDI; N represents the total number of years; $a_0^{(i)}$ a_0 parameter of year i; $\overline{a_0}$ represents the arithmetic mean of a_0 parameter calculated for N years of data (4) (Tsakiris et al. 2007). The standardized RDI includes the standard deviations of each year's a_0 parameter relative to the mean values, thus providing a standardized measure in drought analysis. This index is used to compare and interpret meteorological drought conditions (Zarei et al. 2021).

Spatial interpolation of climate data

Spatial interpolation methods provide convenience for estimating and reproducing values at other unobserved points by using the data of points where observations of a variable are made. For this reason, Kriging method is the most widely used among geostatistical methods that are more preferred in studies. In Kriging method, interpolation surfaces are generated from observations with limited sample (Isaaks and Srivastava 1989). In order to apply these geostatistical methods, it is an important prerequisite to determine the different spatial conditions of observations close to each other (Khorrami and Gündüz 2019). One of the most preferred geostatistical methods to show the spatial distribution of climatic data is Ordinary Kriging (OK) method (Wang et al. 2014). The OK method estimates the values of points with no data by weighted averages of points with nearby data (Hadi and Tombul 2018). The OK method is expressed by the following formula (15) (Hadi and Tombul 2018). The OK method is formulated as follows:

$$\hat{Z}(X_0) = \sum_{j=1}^{N} \lambda_i Z(X_i) \tag{5}$$

Here, the value of the predicted point $\hat{Z}$ at location $\hat{} X_0$ is equal to the sum of the values of each sampled point at location X_i, multiplied by its weight λ_i (Khorrami and Gündüz 2019).

Semivariogram models form the basis of geostatistics and are used to model the spatial dependence of variables (Aksu 2023). The semivariogram model is a technique that measures the half-mean square difference between values against the lag distance or separation of points in spatial autocorrelation (Biswas and Si 2013). There are different types of semivariograms such as spherical, exponential and gaussian. Among these types, the most preferred gaussian method is used to reduce the effect of outliers in climatic parameters by normalizing the data distribution and was also preferred in this study (Hadi and Tombul 2018; Varouchakis 2021).

Results

Precipitation and temperature assessment

The monthly variation of the total annual precipitation between 1991–2022 used in the study is shown in Fig. 3. The average annual precipitation value between 1991–2022 is 1610.9 mm. The months with precipitation above the annual average belong to the months other than July, August and September (Fig. 3). According to the averages of 1991–2022, the highest precipitation in our country is in the Eastern Black Sea region, while the lowest precipitation is in the central parts of Central Anatolia and around Şanlıurfa and Igdir (Fig. 4) (MGM 2022).

The variation of average temperature values by months between 1991–2022 is shown in Fig. 2. The months with the lowest precipitation values in June, July and August

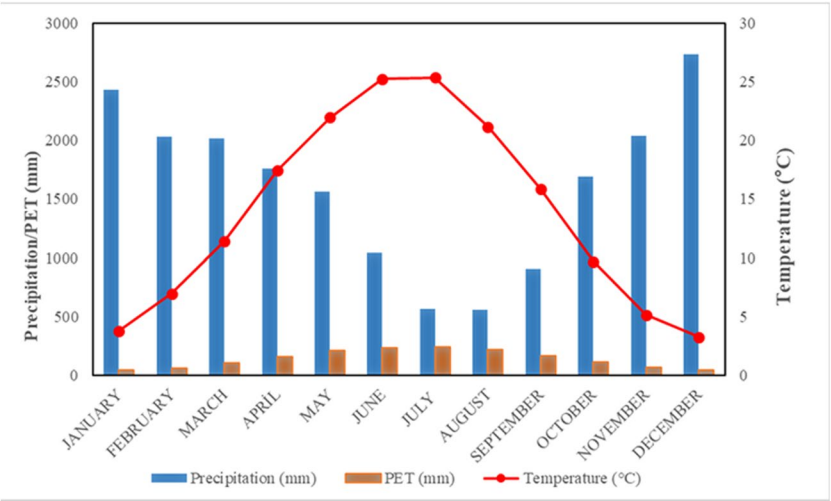

Fig. 3 Graph of monthly average total precipitation, average temperature and average PET values in Türkiye between 1991–2022

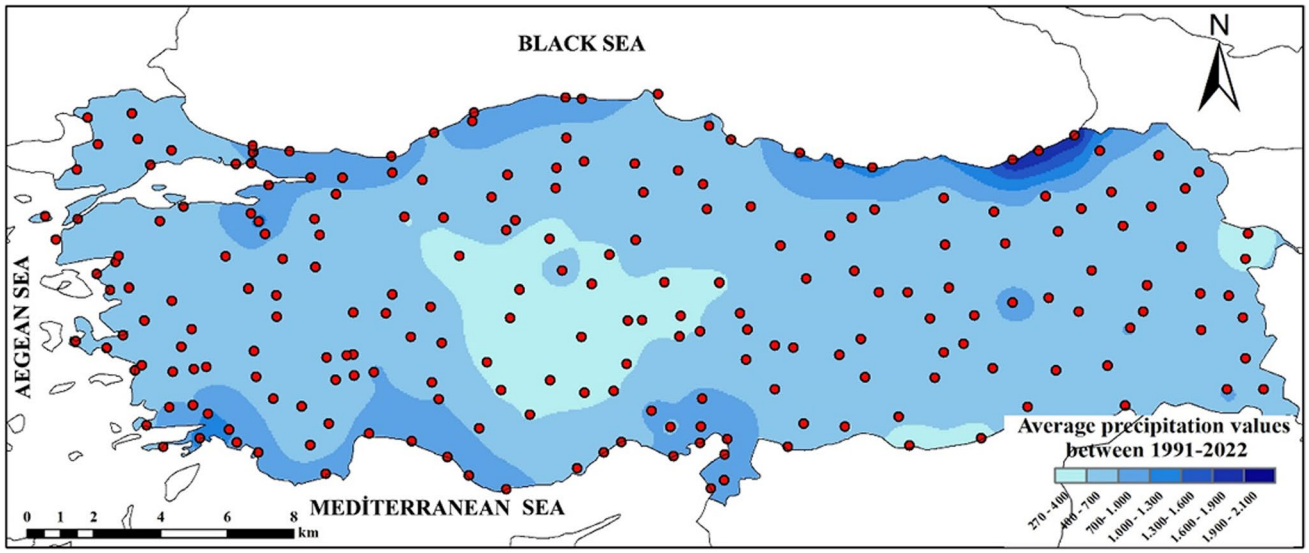

Fig. 4 Spatial variation of annual total precipitation 1991–2022

correspond to both the highest temperature values and the highest evaporation values. The annual average temperature value is 14 °C and the annual average potential evapotranspiration value is 137.5 mm. Above-average temperature values were experienced between March and October between 1991–2022. In the average potential evapotranspiration values, the months above the average are between April and September, when temperature values and evaporation increase (Fig. 3). According to the average temperature values of 31 years used in the study, the highest temperature values extend from the Marmara coast to Southeastern Anatolia (Fig. 5). The lowest mean temperature values are observed in the north–south direction in eastern Central Anatolia and Eastern Anatolia (Fig. 5).

Average frequency values of drought methods by year

In drought analyses, there are class intervals determined to evaluate the time periods when drought periods begin and end and to express drought severity. These class intervals, which are given in Table 1, enable the drought severity to be expressed on a certain scale and facilitate the interpretations made for the region. The high topographic and climatic diversity of the study area causes drought severity to vary. In this context, the average frequency values of drought classes between 1991–2022 were determined. Graphs were created in order to understand the change of the average frequency values calculated for the evaluation of drought classes according to years for all index types. The years with the highest average frequency values in the

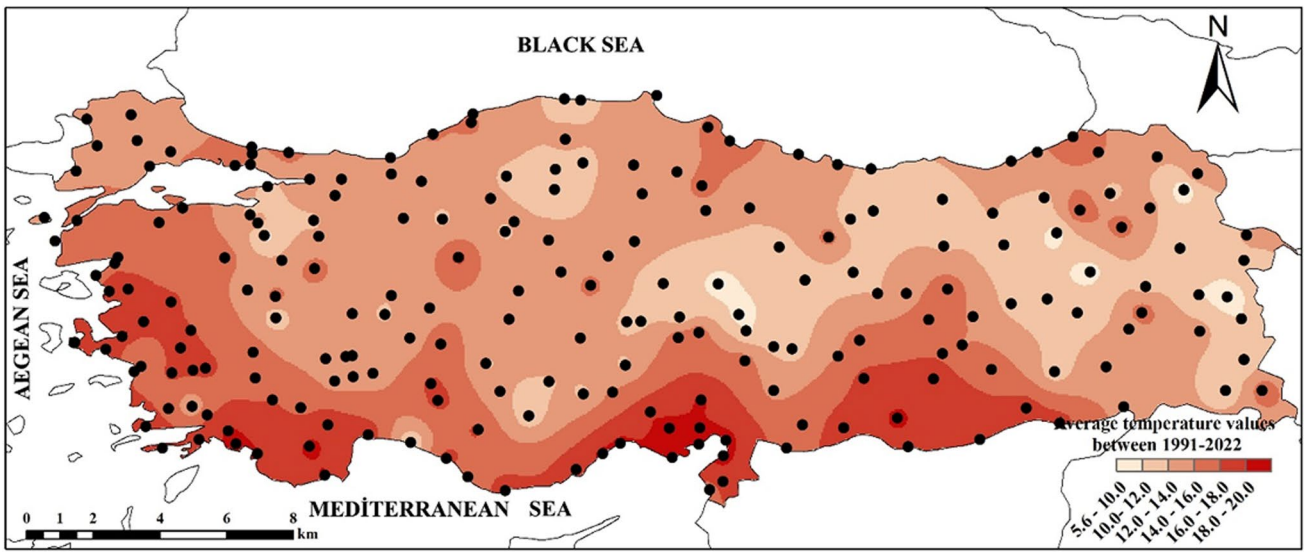

Fig. 5 Average temperature distribution between 1991–2022

graphs were evaluated in detail by comparing the drought analyzes.

In monthly assessments, the highest average frequency values for extremely wet conditions (2.0 and above) and very wet conditions (1.50 to 1.99) in $SPEI_1$ and RDI_1 methods belong to 2022 (Fig. 6). In the monthly SPI_1, extremely wet conditions were observed in 2001, while very wet conditions were identified in 2009 (Fig. 6). These findings emphasize the consistency of different drought indicators in assessing wet conditions and their ability to identify wet periods that vary by year. Moderately wet conditions (1.49 to 1.00), as in other drought classes, have the highest average frequency values in $SPEI_1$ method in 2022, while RDI_1 and SPI_1 indices show the highest frequency value in 2009 (Fig. 6).

While the average frequency values of mild drought conditions (-0.99 to 0.99) were high in 2005 in all three index types, it was determined that the average frequency value was high in 2017 in RDI_1 and SPI_1 indices (Fig. 6). For moderate drought conditions (-1.00 to -1.49), the highest mean frequency values for $SPEI_1$ were in 2016, while for RDI_1 and SPI_1 indices they were in 2008 (Fig. 6). The highest average frequency values of severe dry periods (-1.50 to -1.99) in all indices were observed in 2021. The average frequency value of exceptionally dry conditions (-2.00 and below) was highest in 2001 for all index types (Fig. 6).

In the 3-month analysis evaluations, when analyzed according to drought classes, extremely wet conditions (2 and above) reached the highest average frequency values in $SPEI_3$ and RDI_3 methods in 2022 (Fig. 7). However, in the SPI_3 index, these conditions had the highest recurrence rate in 2002 (Fig. 7). The very wet (1.50 to 1.99) drought class range reached the highest values in 2022 in the $SPEI_3$ and RDI_3 methods, as in the case of extremely wet conditions, while the highest average frequency value was determined in 2009 in the SPI_3 method (Fig. 7). In addition, moderately wet conditions (1.49–1.00) had the highest average frequency value in 2009 for all index types (Fig. 7).

The highest mean frequency value for near normal drought conditions (0.99 to -0.99) belongs to 2005 for all three index species (Fig. 7). The drought class range for moderately drought conditions (-1.00 to -1.49) has a high average frequency in similar years in all three methods. It was determined that moderate drought conditions were more recurrent in 2007, 2008 and 2021 in all methods (Fig. 7). During severe dry periods (-1.50 to -1.99), the highest average frequency value was observed in 2007 and 2020 in all three methods (Fig. 7). Exceptionally drought (-2.00 and below) value intervals were repeated most frequently in 2007 and 2021, similar to each other in the three methods (Fig. 7).

In the 6-month analysis evaluations, the extremely wet (2.00 and above) and very wet (1.50 to 1.99) conditions with the highest average frequency values belong to 2022 for $SPEI_6$ and RDI_6 indices (Fig. 8). As in the other assessments, 2002 has the highest average frequency value for the SPI_6 index. The year with the highest mean frequency value for moderately wet (1.00 to 1.49) conditions is 2009, which is the same year for all three indices (Fig. 8).

Near normal drought (0.99 to -0.99) conditions had the highest mean frequency value in 1996 for all index types (Fig. 8). In moderately drought (-1.00 to -1.49) conditions, the years 2001 to 2021 indicate high values in all indices (Fig. 8). In severely drought (-1.50 to -1.99) conditions, 2021 is a remarkable year with high average frequency values in all three index types (Fig. 8). In exceptionally drought (-2.00 and below) conditions, the years 2021 and 2007 indicate high average frequency values in all three methods (Fig. 8).

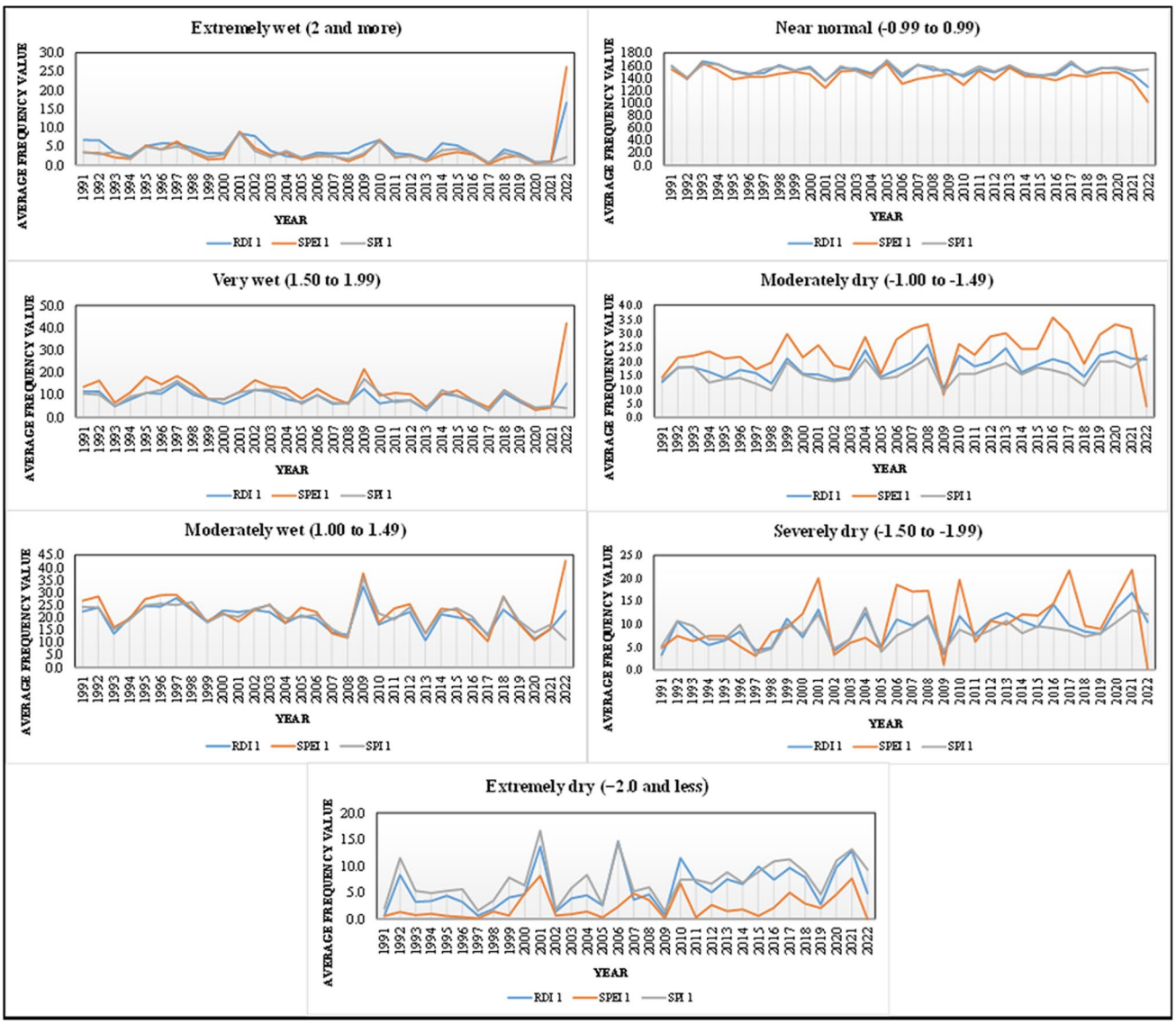

Fig. 6 Representation of average frequency values of drought classes for 1991–2022 for 1-month assessment results

According to the 9-month analysis results, the years with the highest recurrence of extremely wet (2.00 and above) conditions were determined as 2022 for $SPEI_9$ and RDI_9 indices (Fig. 9). Moreover, 2015 is the period with the highest average frequency value for SPI_9 (Fig. 9). The average frequency values for the very wet (1.50 to 1.99) value range were highest in 1998 for RDI9 and SPI_9 indices (Fig. 9). For $SPEI_9$, 2022 is the period in which the average frequency values increase compared to other years (Fig. 9). Moderately wet (1.49 to 1.00) values are observed as conditions repeated in 1998 in all three index types (Fig. 9).

Near normal drought (0.99 to -0.99) conditions were most repeated in 1997 for all indices (Fig. 9). The years in which moderately drought (-1.00 to -1.49) conditions were repeated the most in all three index types were 2001 and 2008, while the extreme drought (-1.50 to -1.99) value ranges were in 2001 and 2021 (Fig. 9). Exceptionally drought (-2.00 and below) conditions were repeated most frequently in 2007, 2014 and 2021 in all three methods (Fig. 9).

In the 12-month analysis of extremely wet (2.00 and above) conditions, the highest average frequency values were reached in 2015 for the SPI_{12} and RDI_{12} indices and in 2022 for the $SPEI_{12}$ index (Fig. 10). One of the years in which very wet (1.50 to 1.99) conditions persisted, 1998, was observed in all three index types (Fig. 10). The highest average frequency values occurred in 2015 for the RDI12 and SPI_{12} methods and in 2022 for the $SPEI_{12}$ index (Fig. 10). Moderately wet (1.49 to 1.00) conditions were repeated in 1998 for all three index types (Fig. 10).

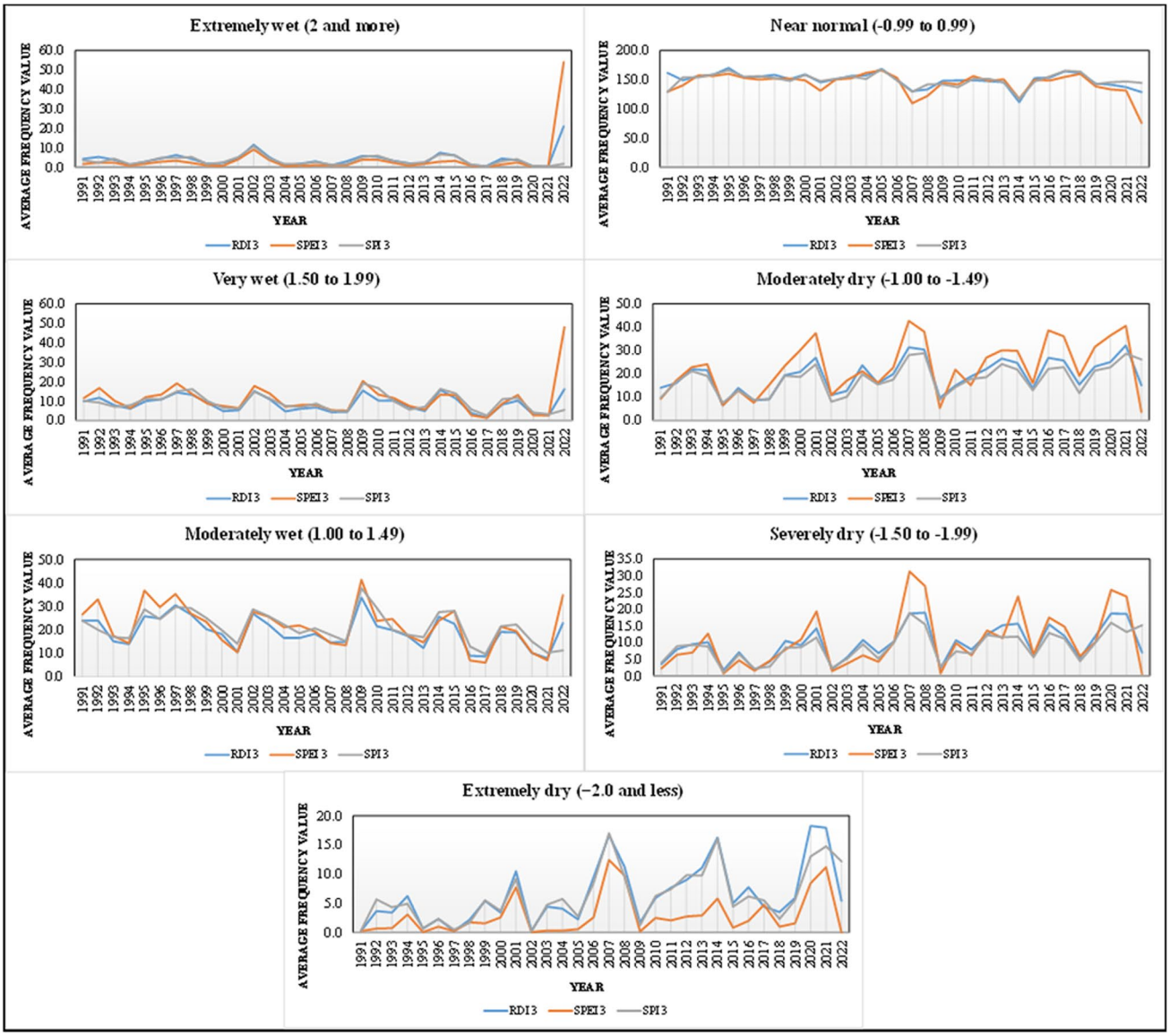

Fig. 7 Representation of the average frequency values of drought classes for the period 1991–2022 for the 3-month assessment results

Unlike the wetity classifications, near normal drought (0.9 to -0.99) conditions reached the highest mean frequency value in all methods in 1997 (Fig. 10). Moderately drought conditions (-1.00 to -1.49) had the highest frequency in 2001 in all indices (Fig. 10). In 2014 and 2021, it was observed that severe drought (-1.50 to -1.99) value ranges had the highest average frequency values in all methods (Fig. 10). It was determined that extreme conditions (-2.00 and below) had high average frequency values in all methods in 2007, 2014 and 2021 (Fig. 10).

The years of effective and severe water deficit in most of Türkiye are noteworthy in the recurrence of drought severity in average frequency values. In 1 and 3-monthly evaluations, the average frequency value of severe drought values in 2001, 2005, 2007, 2008, 2016, 2017, 2020 and 2021 is high. In the short-term drought indices, the effect of meteorological drought, which was combined with the summer drought in 2013, which increased in severity after 2012, and the drought of 2001, 2007–2008, which was the longest drought in Türkiye (Türkes and Erlat 2003; Türkes 2020b) . In the 6, 9 and 12-month indices, it was determined that the average frequency values in 1996–1997, 2001, 200–2008, 2014 and 2021 were high in severe droughts. This indicates that long-term drought indices reflect the years corresponding to prolonged severe drought in Türkiye.

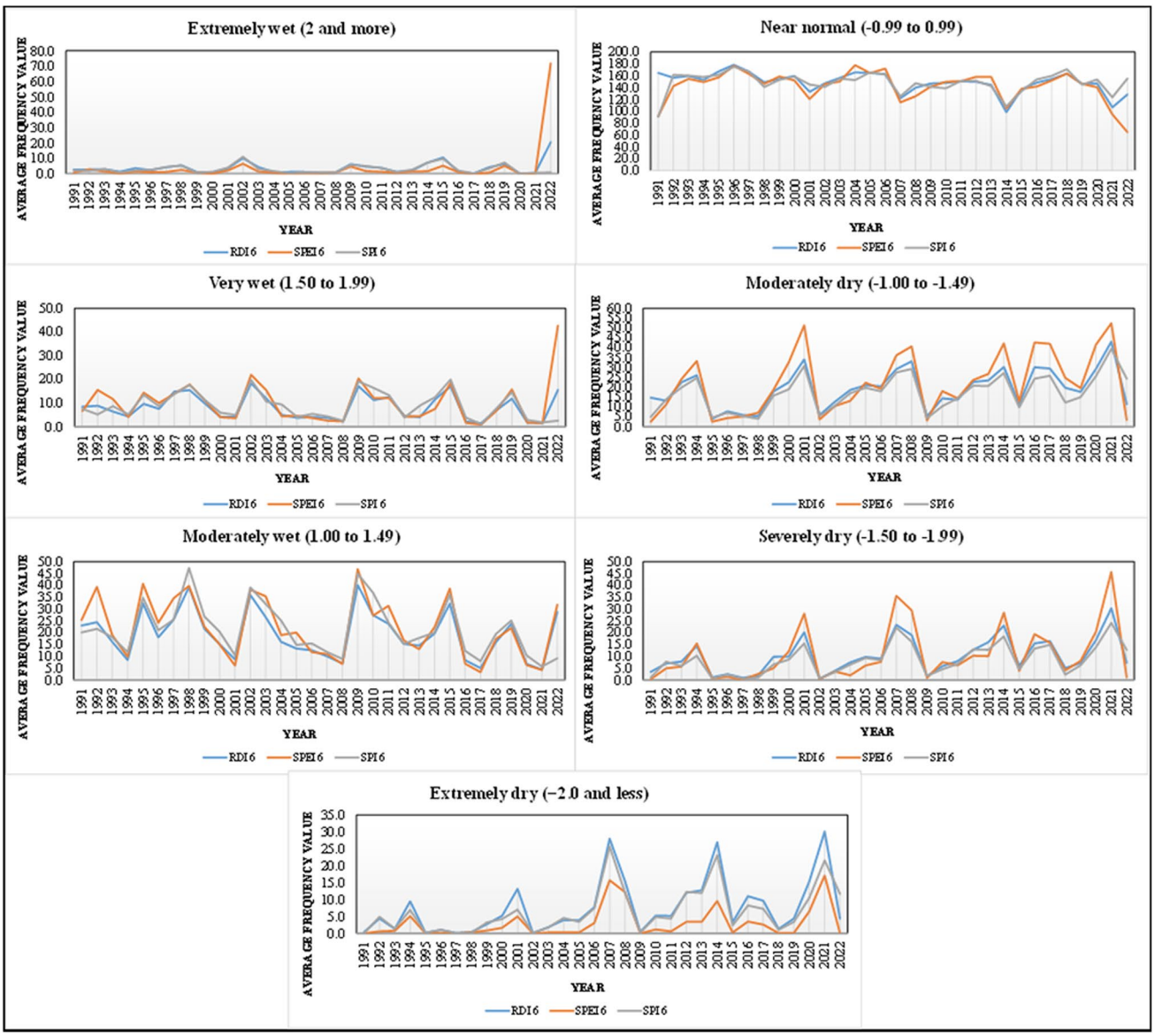

Fig. 8 Representation of the average frequency values of drought classes for the period 1991–2022 for the 6-month assessment results

SPI, SPEI and RDI methods 1-month evaluation analyses

In drought indices, 1-month periodic assessments are based on short-term monthly precipitation distribution. Short-term soil moisture, especially during the growing season of plants, is closely related to plant stress and meteorological drought (WMO 2012). In 1-month periodic evaluations, the years 1994, 2003, 2006, 2007, 2010, 2014, 2015, 2017 and 2020 were the years with the highest drought values in SPI_1 method. In the RDI_1 method, the highest drought values belong to the years 1994, 2006, 2010, 2012, 2015, 2016 and 2017. In the $SPEI_1$ method, the years 1999, 2001, 2007, 2008, 2009, 2016, 2017 and 2019 are the years with the highest drought values. The spatial variation of these years in the study area was mapped for each month. In addition, by comparing all indices, the driest/moist years for each month and their spatial distribution in the study area are briefly summarized below with the reasons.

The years and areas with the highest drought values in January, February, March and April are shown in Fig. 11. In January, SPI_1 (-6.08 to -1.29) and RDI_1 (-4.72 to -1.28) indices show high drought values in the southeastern part of the study area, while $SPEI_1$ (-4.54 to -1.28) index shows high drought values in the northern part of the study area. In the winter season of 2010, when the highest drought values were observed in January in SPI_1 and RDI_1 indices, the above-average temperature values caused the drought severity in

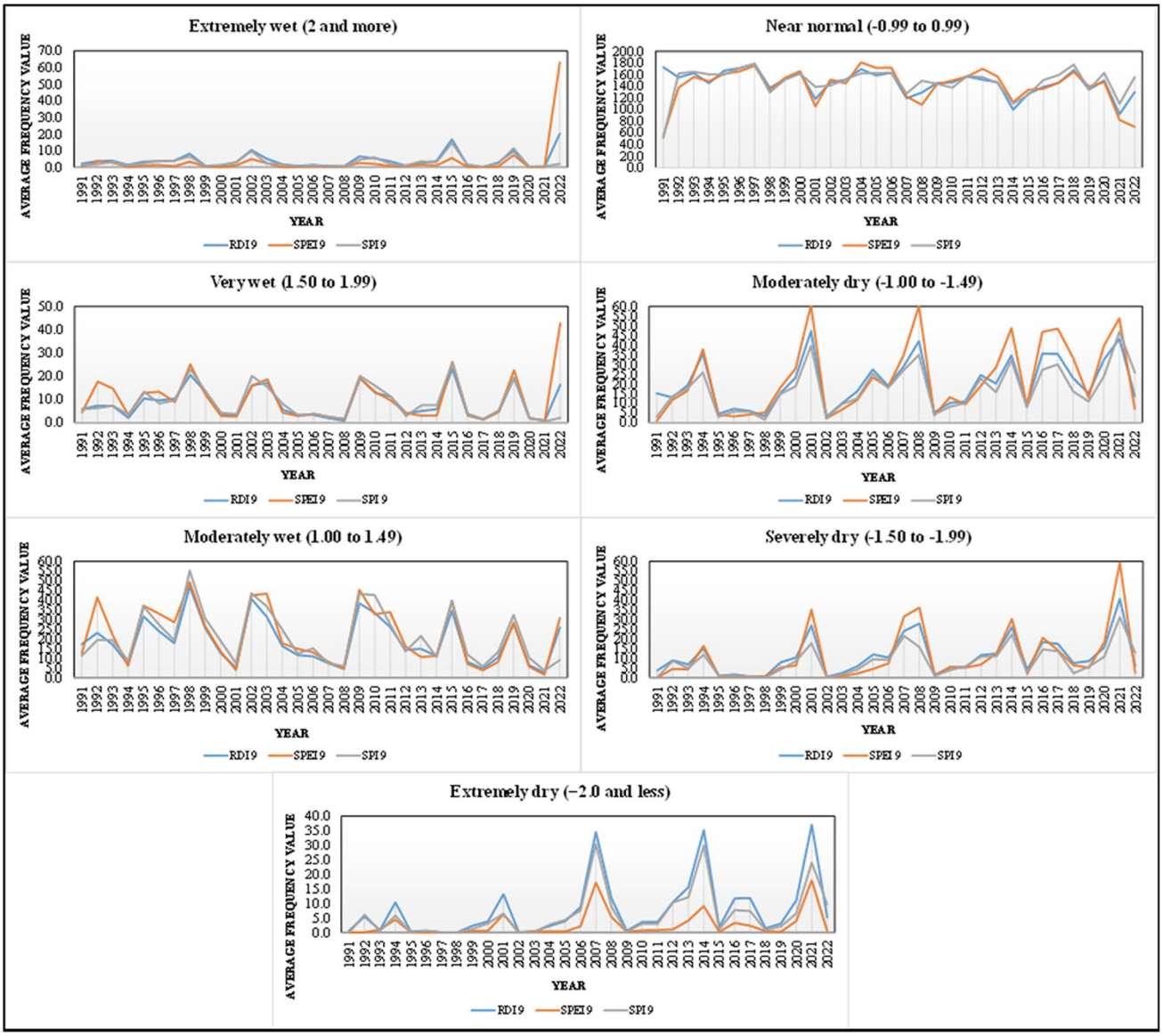

Fig. 9 Representation of the mean frequency values of drought classes for the period 1991–2022 for the 9-month assessment results

the southeastern part to increase (Güler and Erlat 2023). The fact that 2010 was the warmest winter season explains the high drought severity in the stations in this region for both index types. In the $SPEI_1$ index, especially the winter precipitation in the form of snow in 2014 caused exceptionally drought values in the northern parts of the study area (Fig. 11) (Simsek et al. 2013). While drought values in February were high in SPI_1 (-6.05 to -0.83) and RDI_1 (-4.83 to -0.62) methods in almost all of the study area, high drought values in $SPEI_1$ (-3.02 to -0.63) index were observed in the inland areas (Fig. 11). The increasing trends in drought observed in SPI_1 and RDI_1 indices in February 2017 were detected during the period from December to September, which also affected inland Türkiye, eastern and western Iran, northern Iraq and Syria, western Jordan, and Israel (Sahour et al. 2020). The increasing trend in drought is particularly associated with reduced precipitation and increased potential evapotranspiration.

While the drought severity in March was high in the western part of the study area in SPI_1 (-5.64 to -1.12), it increased in the eastern part of the study area in RDI_1 (-4.37 to -0.86) and $SPEI_1$ (-3.22 to -0.38) indices. In the SPI_1 index of March, it is seen that the drought severity in 2007 increased especially with the below normal fall and winter precipitation starting from 2006 until December 2008 (Türkes 2012). Consistent with the results of the study, this aridification trend was most effective in the Aegean Mediterranean, Marmara and Southeastern

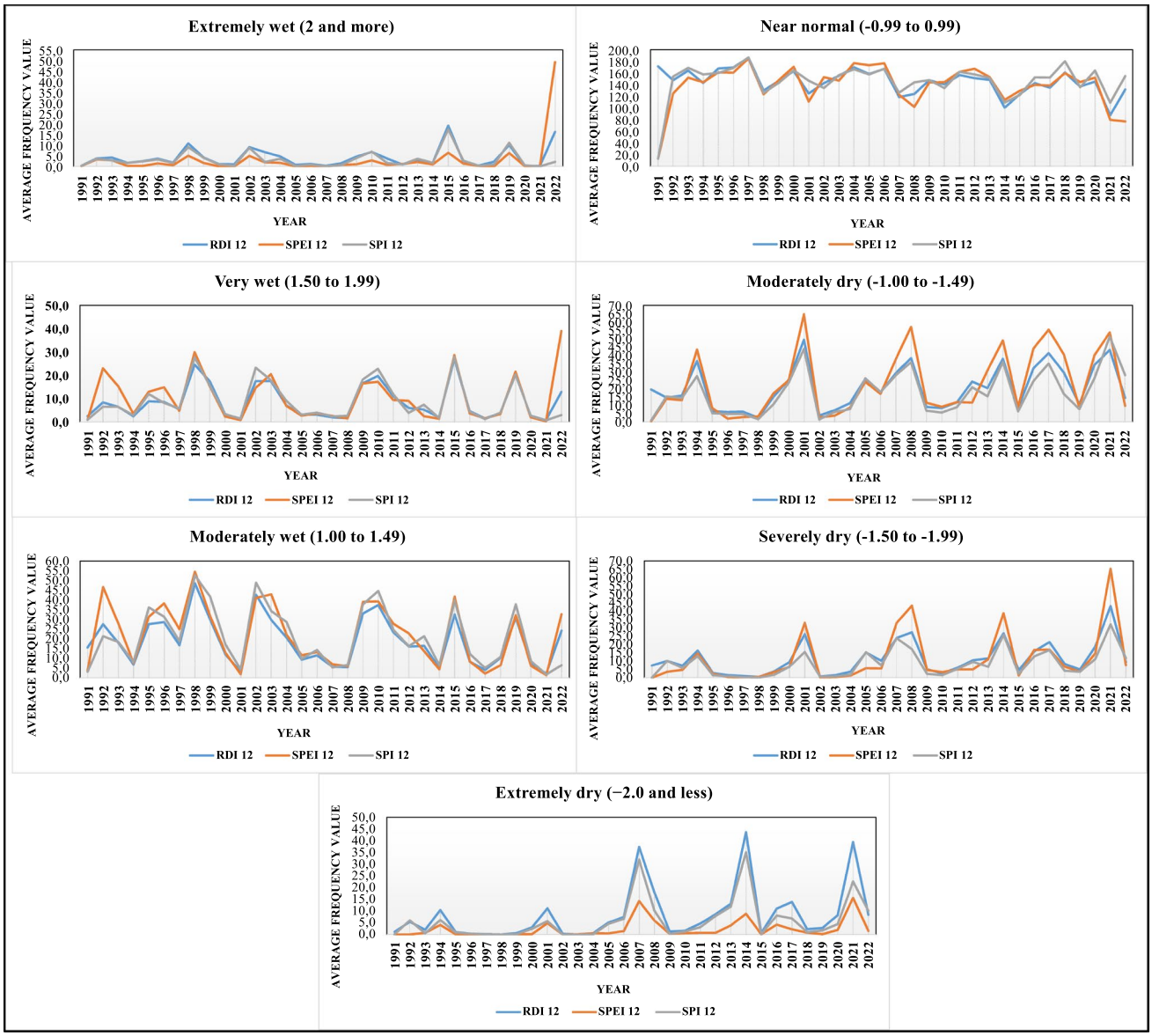

Fig. 10 Representation of the average frequency values of drought classes for the period 1991–2022 for the 12-month assessment results

Anatolia in Türkiye (Türkes 2007). In the spring season, March, especially the temperature increase trends observed since 2001 explain the increasing drought severity in SPI_1 and RDI_1 indices in 2012, 2015 and 2018 (Fig. 11). For SPI_1 (-4.82 to -0.94), the drought severity in April was higher in the western part of the country and for $SPEI_1$ (-3.70 to 0.00) in the eastern part of the country, while for RDI_1 (-4.82 to 0.00), the drought severity increased from the western part to the northeast (Fig. 11). For the $SPEI_1$ index, drought severity was high from February to April 2008 (Fig. 11). The year 2008 was a period of high drought severity in Türkiye with increasing temperatures and decreasing precipitation. During this period, especially in agricultural production, the country experienced serious production losses in crops such as wheat, corn, paddy, sunflower and potato (Taskın et al. 2022).

In January, exceptionally wet conditions with wet conditions of 2 and above were observed in RDI_1 (4.51) in 2008 in the eastern part of the study area, SPI_1 (3.42) in 2015 in the south of the Marmara Sea and $SPEI_1$ (2.58) in 2016 in Central Anatolia. The southward expansion of the wet northern Black Sea belt, especially between 2015 and 2020, caused exceptional wet conditions (Kömüscü et al. 2022). In February assessments, the highest wet conditions were observed in RDI_1 (3.89) in the south of the Black Sea in 2011, SPI_1 (3.10) in the east of the study area in 2004 and $SPEI_1$ (2.73) in the south of the study area in 2022. According to the index types, the highest precipitation values in 2011 and 2022 are

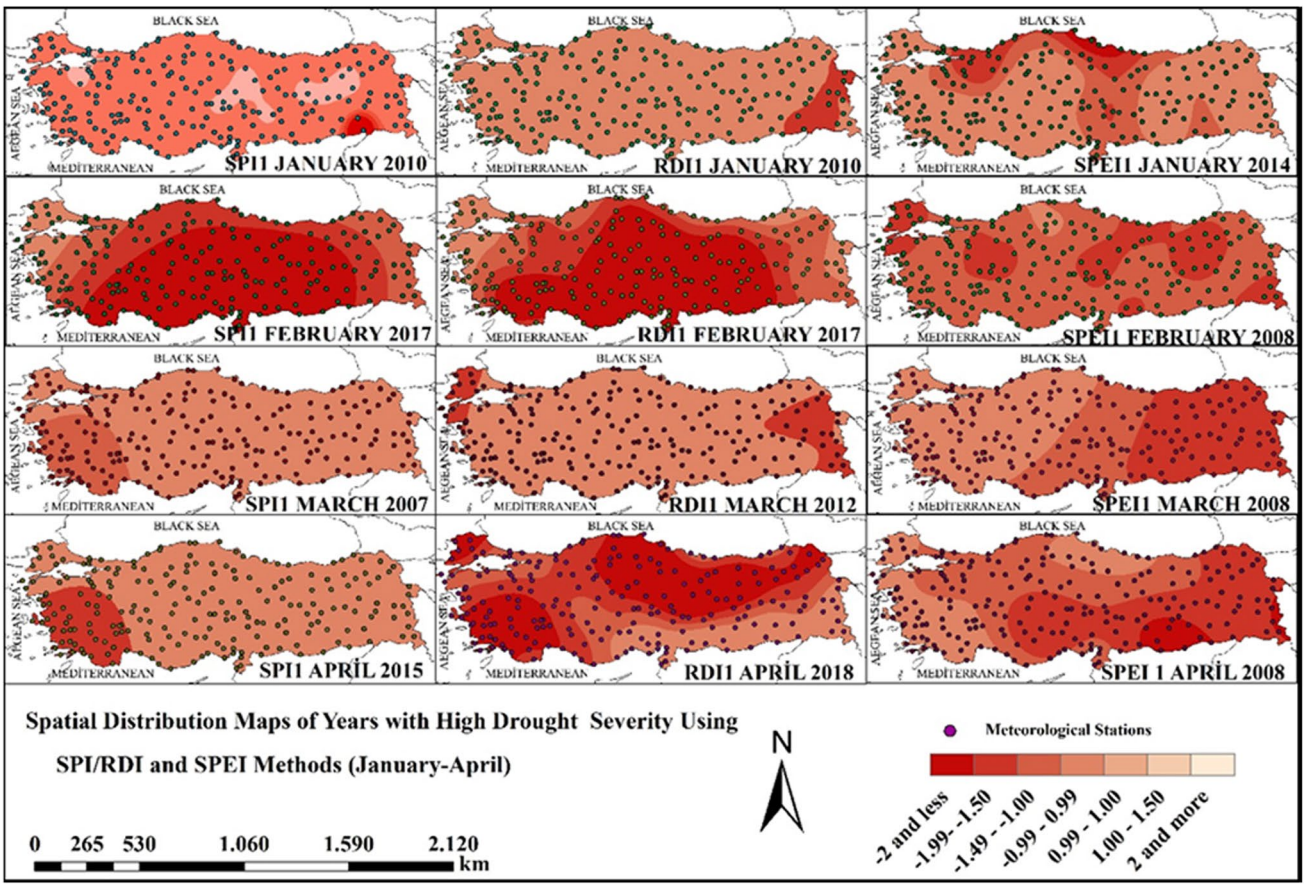

Fig. 11 Graphs of the years (January-April) in which the highest droughts were determined for each month of the 1-month analysis in SPI, SPEI and RDI methods

observed on the Black Sea coast and in the southern part of the study area as a result of the topographic effect due to the mountains extending parallel to the coastal area. March wet conditions are highest in Central Anatolia in 2015 with RDI_1 (4.37) and SPI_1 (3.91) and in the east of the study area in 2003 with $SPEI_1$ (2.60). The highest April wet conditions in RDI_1 (5.42) were in the northwest of the study area in 2013. SPI_1 (3.81) in 2012 in the western part of the study area and $SPEI_1$ (2.62) in 2015 in Central Anatolia. The fact that the rainy period of Central Anatolia coincides with the months in the spring season causes high wet conditions.

The years and areas with the highest drought values in May, June, July and August are shown in Fig. 12. In the drought assessments in May, SPI_1 (-4.40 to -0.89) and $SPEI_1$ (-3.54 to 0.00) indices show moderate drought conditions across Türkiye, while the highest drought value in RDI_1 (-5.44 to -0.75) index is observed in the northeast (Fig. 12). May is the month with the most severe warming after April 2008, and the increase in drought severity with increasing temperatures, especially after 2003, is remarkable (Güler and Erlat 2023). The SPI_1 method, in which 2014 is represented by severe drought, is in parallel with other studies (Simsek et al. 2013). RDI_1 2016 in May and $SPEI_1$ 2017 in May show that the impact area of drought has expanded with the effect of increasing warming after 2008. In June, SPI_1 (-4.99 to -1.27) shows high drought severity in the south, while $SPEI_1$ (-3.92 to 0.00) shows an increase in drought severity in the coastal area from north to south (Fig. 12). Unlike the other indices, RDI_1 (between -3.90 and -1.02) indicates normal drought conditions in the eastern parts and wet conditions in the interior.

SPI_1 in July (-3.42 to -1.80) and August (-4.63 to -1.78) shows that the study area is generally dominated by normal drought values. However, the RDI_1 index shows an increase in drought severity in the northeast in July (-3.44 to -0.87) and in the north in August (-4.18 to -1.11) (Fig. 12). In the $SPEI_1$ index type, drought severity increases in the inland areas in July (-3.22 to 0.00), while this situation shifts towards the southeast in August (-3.83 to -1.05) (Fig. 12). The positive anomaly values observed in summer season temperatures after 2010 are associated with the mega-temperatures affecting Türkiye, with Russia in the center. The effect of this temperature increase on aridity is seen in RDI_1 index in June and July 2015 (Fig. 12). In $SPEI_1$, July

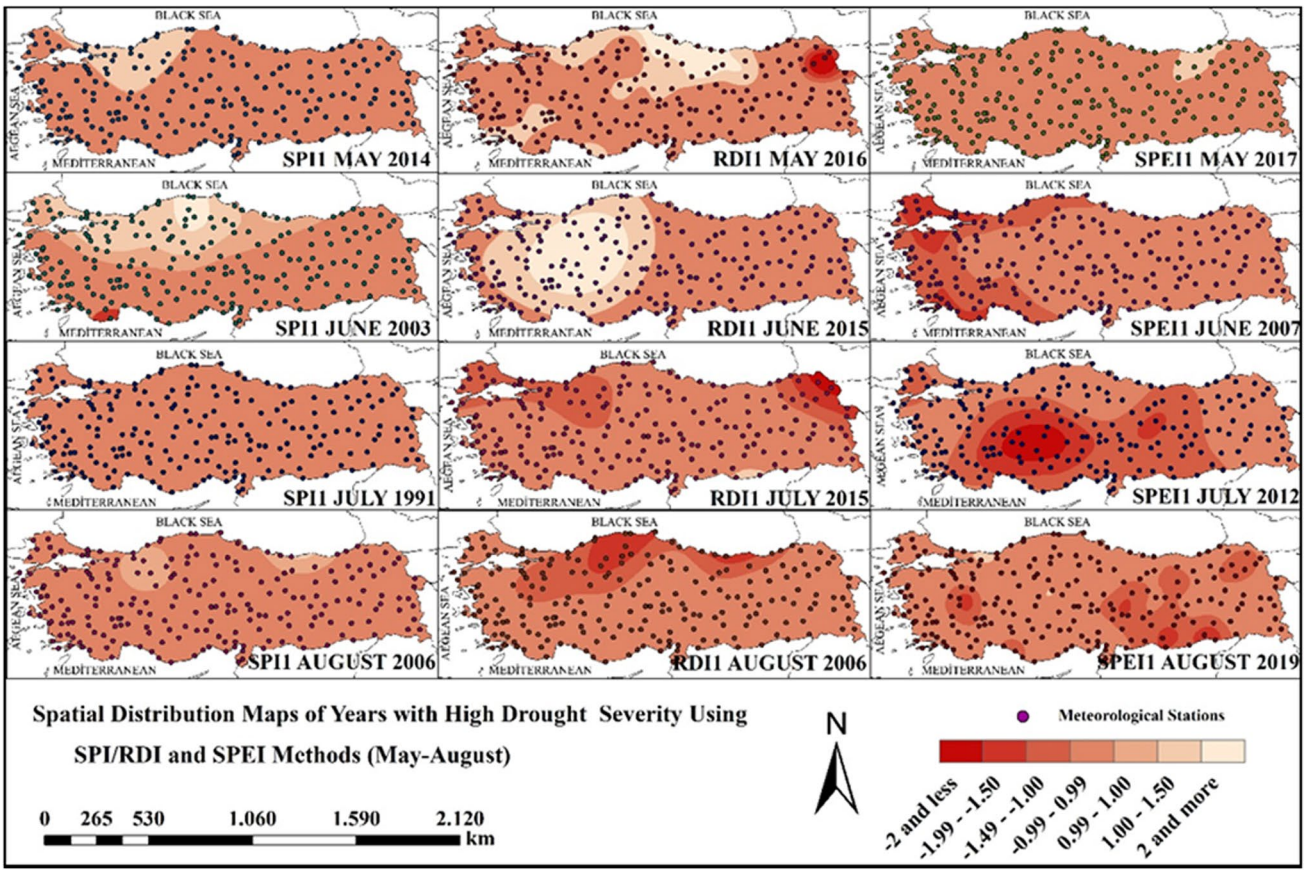

Fig. 12 Graphs of the years (May–August) in which the highest droughts were determined for each month of the 1-month analysis in SPI, SPEI and RDI methods

2012 and August 2019 show the impact of increasing temperatures on drought. In June, SPI_1 2003 and $SPEI_1$ 2007 are the years when the highest drought severity is repeated. SPI_1 1991 in July and 2006 in August are the years with the highest drought severity in SPI_1 and RDI_1 indices. It was determined that the drought severity, which was especially effective starting from 2006 until 2008, caused the highest drought values to be seen in these indices in the summer months (Türkes 2012; Akbas 2014).

In 2022, the highest wet conditions for all methods were determined in the Black Sea coastal region. RDI_1 (5.55) was measured in the Eastern Black Sea station, while $SPEI_1$ (2.94) in the Central Black Sea and SPI_1 (3.00) in the Western Black Sea were the highest. When ranked according to the wet conditions in July, the highest value was obtained in the RDI_1 (4.46) method measured in the Eastern Black Sea region in 2016. Then, the second highest value was SPI_1 (3.56) calculated in the eastern part of the study area in 2009. The lowest wet conditions were observed in 2022 with a value of 3.41 obtained with the $SPEI_1$ method applied in the coastal part of the Aegean Sea. The highest wet conditions in August in 2022 were RDI_1 (3.64) in the west of the study area and $SPEI_1$ (3.08) in the southwestern coastal area of the Aegean Sea. In the SPI_1 (2.75) method, wet conditions were high in the south of the Marmara Sea in 1997.

The years and areas with the highest drought values in September, October, November and December are shown in Fig. 13. In September, drought values in SPI_1 (between -4.46 and -1.38) and RDI_1 (between -3.35 and -1.01) indices are high in the northern and northwestern parts. In $SPEI_1$ (-3.09 to 0.00), the highest drought values are observed in the northern and eastern parts (Fig. 13). The warming trend that started in the first half of the 1990s has gradually increased since the twenty-first century. The highest drought values were determined in SPI_1 and RDI_1 indices in September 1991 and in $SPEI_1$ index in December 1998. In Türkiye, the period when a significant warming trend is observed belongs to the fall months. The warming trend seen especially since 2010 causes drought to recur more frequently. With the effect of increasing temperature and evaporation, the highest wet conditions in the $SPEI_1$ index is in 2017 as in other studies (Güler and Erlat 2023). In October, it is observed that the drought severity increases from south to north and east in the SPI_1 (-6.10 to -0.39) and RDI_1 (-4.62

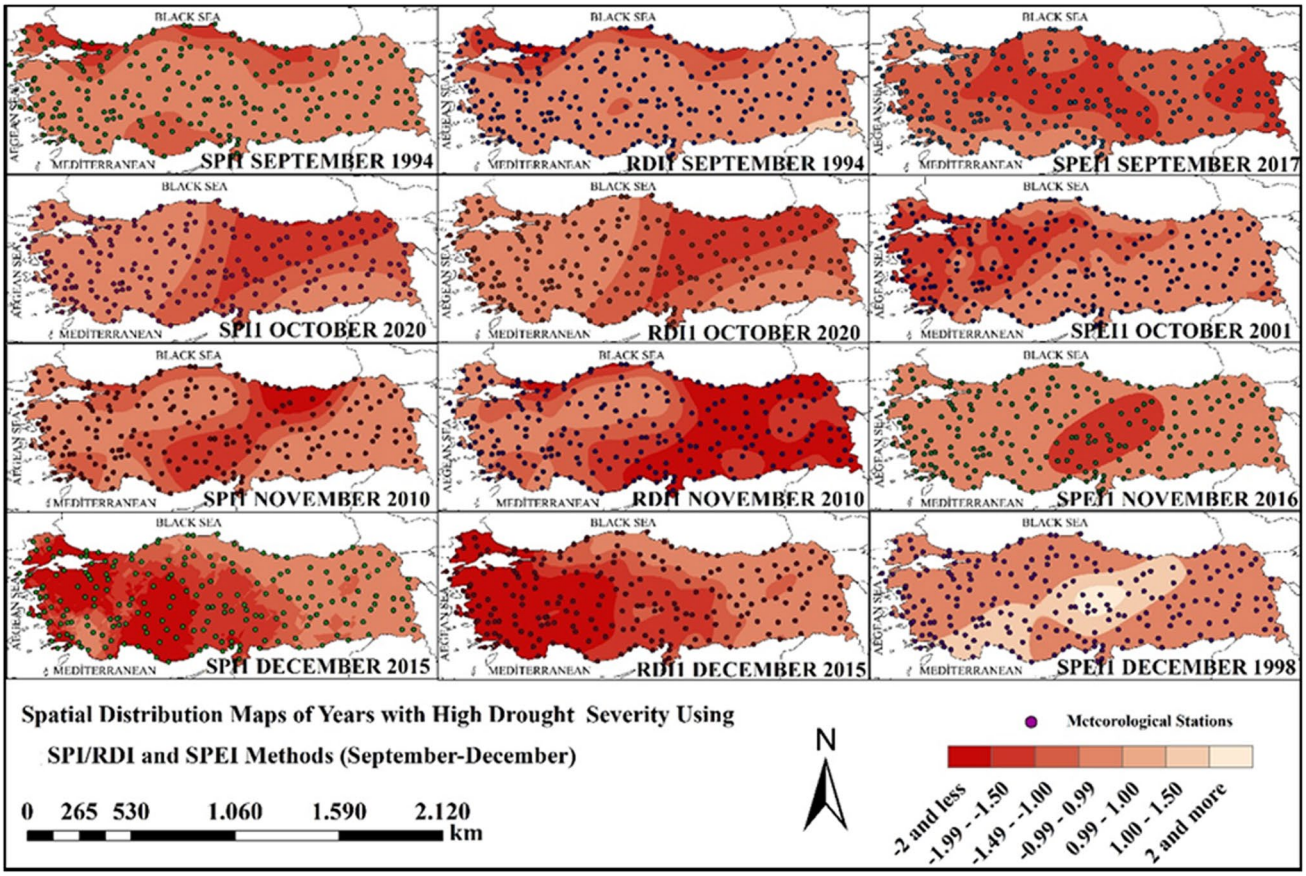

Fig. 13 Graphs of the years (September-December) in which the highest droughts were determined for each month of the 1-month analysis in SPI, SPEI and RDI methods

to -0.38) indices, while the drought severity increases in the western parts of the $SPEI_1$ (-3.04 to -0.59) index (Fig. 13). In October, SPI_1 and RDI_1 show the highest drought severity in Türkiye in the fall season of 2020.

In November, drought severity in SPI_1 (-4.89 to -0.75) index has the highest values from south to north. RDI_1 (-4.25 to -0.81) has the highest drought values from inland to the east (Fig. 12). $SPEI_1$ (-2.53 to -0.99) has high drought values only in inland areas. In December, SPI_1 (-5.56 to -0.19) and RDI_1 (-4.61 to -0.23) indices have similarly high drought values in the western and southern parts, while $SPEI_1$ (-2.39 to 0.00) also has high drought values in the eastern parts (Fig. 13). In November, drought intensity is high for SPI1 and RDI1 in 2010. In December, SPI1 and RDI1 indices show an increase in drought values for 2015. The stations in the east and southeast, where drought severity was the highest during the analysis period, are located in both topographic conditions and continental climate zone. In addition, the fact that different types of air masses are effective according to the months causes the drought severity to increase. The stations in the continental climate regions are closed basins and local differences in the climate in mountainous areas and basins and the variability in the distribution and regime of precipitation increase the vulnerability to drought (Bahadır 2013; Kale 2021).

In September 2022, high wet conditions in RDI_1 (4.48) and $SPEI_1$ (2.70) were determined in the east of the study area. In the SPI_1 (2.81) method, the wet conditions is high in the northern part of the study area in 2014. The highest October wet conditions at the stations in the east of the study area belong to RDI_1 (4.55) in 2022 and SPI_1 (3.11) in 2015. In the $SPEI_1$ (2.55) method, the highest wet conditions in Central Anatolia in 2010 are noteworthy. RDI_1 (5.10), where wet conditions were highest in November, was determined in the east of the study area in 2022. In 2001, the highest wet conditions for both $SPEI_1$ (2.72) and SPI_1 (3.33) belong to the stations in the southwestern and southern parts. The highest wet conditions in December were determined as RDI_1 (4.00) in 1994 and SPI_1 (3.06) in 2013 at the stations in the east of the study area. However, in the $SPEI_1$ (2.57) method, the wet conditions were highest in 2014 in the southwest of the study area.

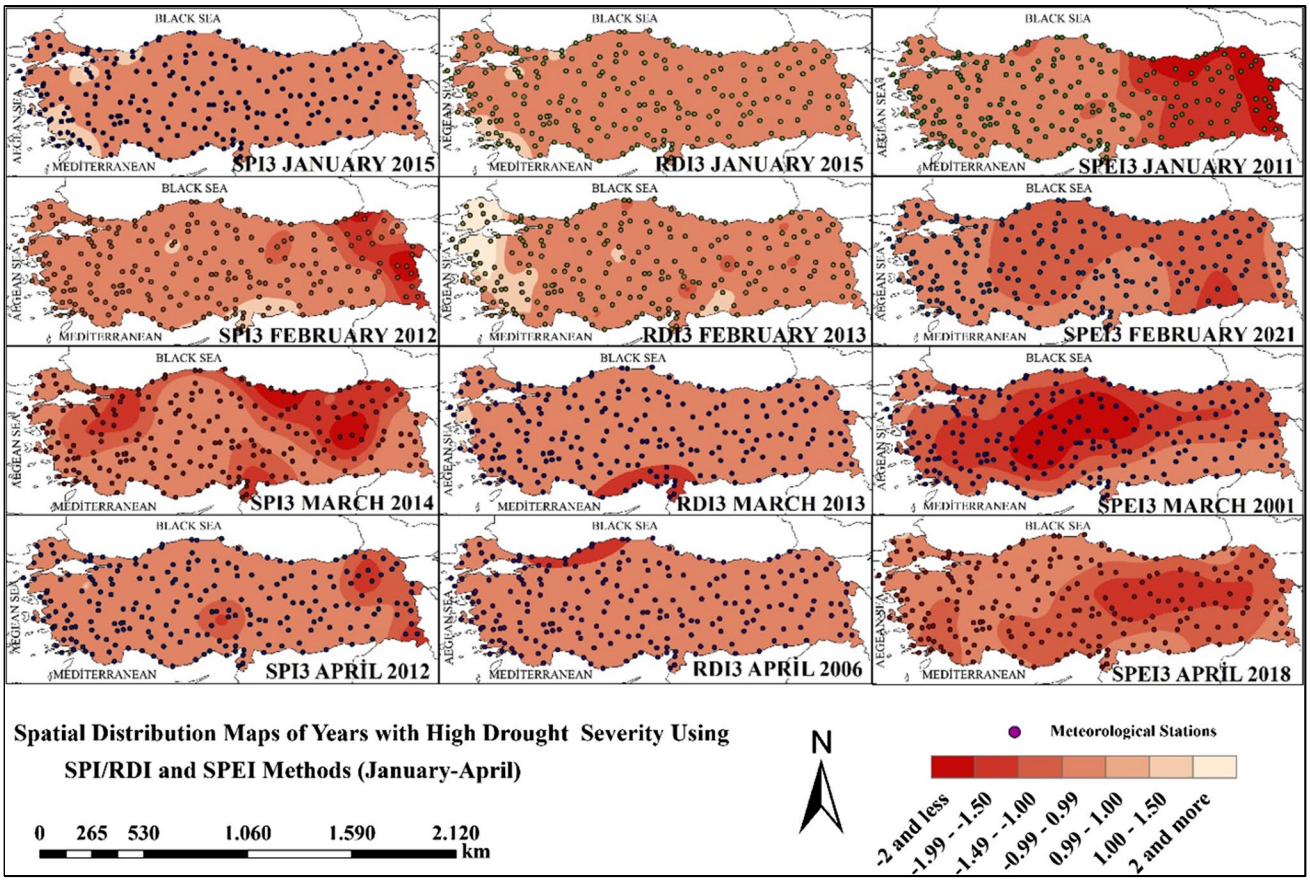

Fig. 14 Graphs of the years (January-April) in which the highest droughts were determined for each month of the 3-month analysis in SPI, SPEI and RDI methods

SPI, SPEI and RDI methods 3-month evaluation analyses

In 3-month assessments, it enables the comparison of precipitation in certain 3-month periods with the same 3-month precipitation for all years in the historical record (WMO 2012). In the SPI method, the highest drought values were determined in 2006, 2007, 2008, 2011, 2012, 2014, 2015 and 2022 in the 3-month analysis. In the RDI $_3$ method, the highest drought values are found in 2006, 2008, 2012, 2013, 2015 and 2021. $SPEI_3$ method shows the highest drought values in 1998, 2001, 2007, 2011, 2017, 2018, 2020 and 2021. The months of these years are mapped and the spatial variation of 3-month drought is shown. By comparing all indices, the driest/moist year and stations for each month are briefly summarized below.

The years and areas with the highest drought values in January, February, March and April are shown in Fig. 14. In January, it is seen that normal drought values are dominant in SPI_3 (-5.72 to -0.94) and RDI_3 (-5.47 to -1.07) indices throughout Türkiye. However, in $SPEI_3$ (-3.55 to -0.88), drought severity is shown to be high in the eastern part (Fig. 14). There are significant decreasing trends in annual precipitation and especially in winter precipitation in the Eastern Mediterranean basin and in general. This situation is observed to increase the severity of drought with the decrease in the frequency of mid-latitude and Mediterranean low pressures, which are especially effective in the winter season, and the increase in high pressure conditions in 2015 (Topcu 2022). This is supported by the results of SPI_3 and RDI_3 in January in Fig. 14. Especially in $SPEI_3$ index, the drought values that intensified in 2011 can be interpreted with the decrease in precipitation in the winter season and the increase in the effect of high pressure conditions in the region. In February, SPI_3 (-5.71 to -0.75) shows increased drought severity in the eastern part of the study area, while RDI_3 (-5.06 to -0.80) shows normal drought values throughout the study area. In $SPEI_3$ (-3.14 to -093), high drought values are observed in the southeastern part in February. In March, the areas with high drought severity differ in all index types (Fig. 14). Drought intensity increased in the northwestern and eastern parts in SPI_3 (-5.62 to -0.91), in the south in RDI_3 (-5.08 to -4.87) and inland in $SPEI_3$ (-3.67 to -0.62). In April, drought intensity was high in the eastern

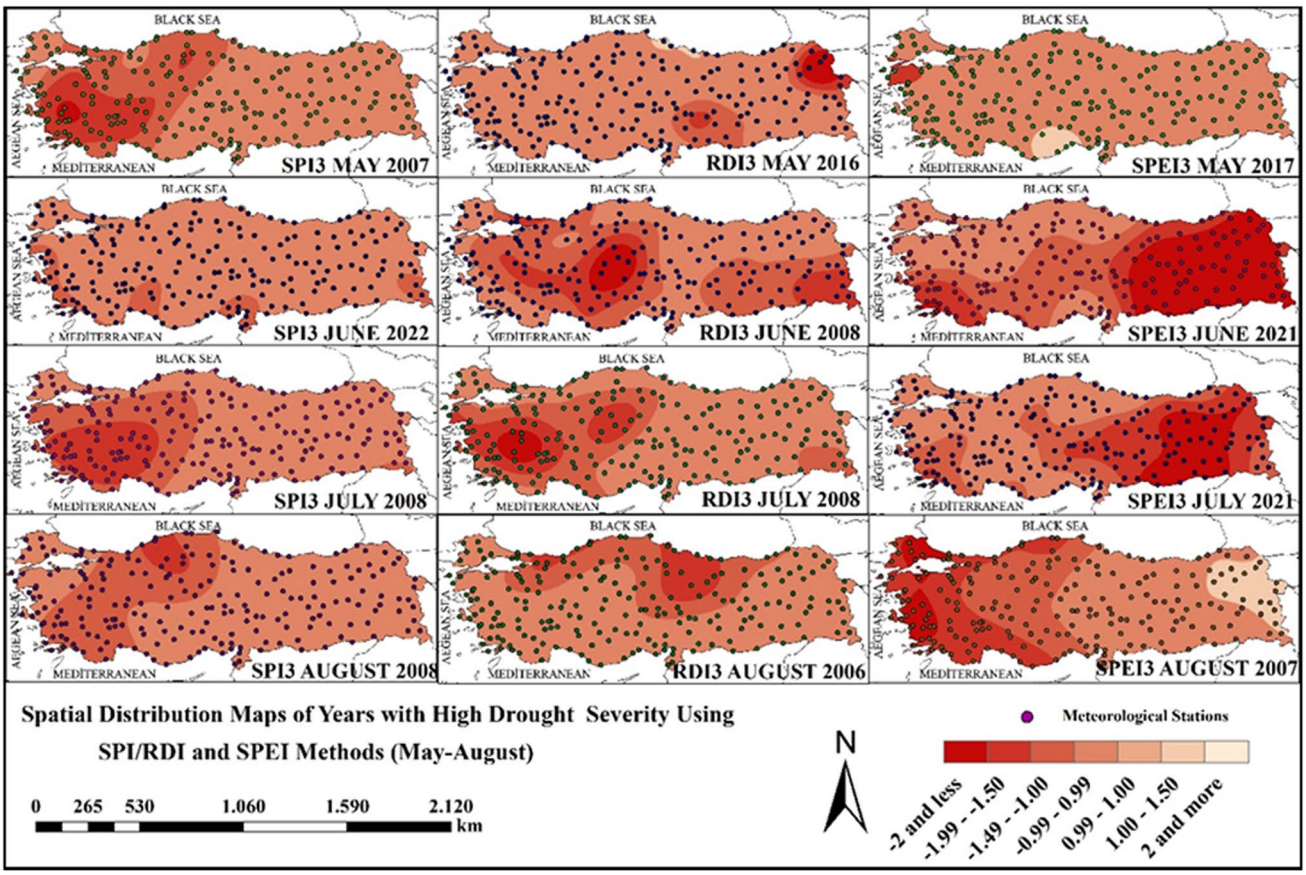

Fig. 15 Graphs of the years (May–August) in which the highest droughts were determined for each month of the 3-month analysis in SPI, SPEI and RDI methods

parts in SPI_3 (-5.38 to -0.75) and $SPEI_3$ (-3.00 to -0.31), while drought values increased in the Western Black Sea in RDI_3 (-5.10 to -0.54).

The increase in the drought values of SPI_3 in February and April 2012 in the eastern parts of the country is due to the effect of continental climate and at the same time, precipitation values below normal in this period (Simsek et al. 2012). With the effect of this drought, losses were observed in crops such as wheat, barley and sugar beet (Simsek et al. 2012). RDI_3 The drought in February and March 2013 can be evaluated with the increase in seasonal average temperatures since 2010 (Güler and Erlat 2023). The 2014 severe drought SPI_3 was observed in March. The drought covering the 2013–2014 agricultural year was severe, resulting in losses in agricultural yields (Simsek et al. 2013; Ozelkan et al. 2016). The 23.6% decrease in precipitation in February 2021 compared to normal $SPEI_3$ represents a severe drought period effective in the whole country (Taskın et al. 2022). The highest increase in annual average temperatures was in 2018, and the increase in evaporation intensity due to this situation is represented by the increased drought severity in the terrestrial regions and the entire study area in April $SPEI_3$ (Fig. 15). After 2000, increasing temperature and decreasing precipitation values affect severe drought in March $SPEI_3$ and April RDI_3.

In January, 2002 was the year with the highest wet conditions in SPI_3 (3.70) and $SPEI_3$ (2.94) methods and wet conditions was high at stations in Central Anatolia. In the RDI_3 (3.52) method, it was determined that the wet was the highest in the east of the study area in 2014. In RDI_3 (4.42) and $SPEI_3$ (2.87) methods, the highest wet conditions in February were in the Black Sea coastal area in 2022. In SPI_3 (3.58) method, the wet conditions is high in the south of the Marmara Sea in 2015. According to the wet conditions, the highest wet conditions was obtained in March in 2022 with RDI_3 (5.54) in the east of the study area and $SPEI_3$ (2.67) in the western Black Sea coastal area. The lowest wet conditions were observed in Central Anatolia in 2015 with SPI_3 (3.85). April wet conditions in the northwest of the study area in 2013 were high in SPI_3 (5.03) and RDI_3 (5.56) methods. The $SPEI_3$ (2.68) method shows the highest wet conditions in Central Anatolia in 2015.

The years and areas with the highest drought values in May, June, July and August are shown in Fig. 15. The

effects of the 2007–2008 period of severe drought in Türkiye are seen in SPI_3 in May, RDI_3 in June and SPI_3 and RDI_3 indices in July. In the May assessments, it is observed that normal dry conditions prevailed across Türkiye in all three index types (Fig. 15). In the May map of SPI_3 (-4.93 to -0.85), drought increased in the western part and in the $SPEI_3$ (-3.20 to -0.47) index in the west coast. However, in the RDI_3 (-6.06 to -1.09) May map, drought is higher in the southeastern and northeastern parts. The drought effect seen in the entire study area in the RDI_3 and SPI_3 indices in May in 2016–2017 was due to the effect of the heat wave centered in Russia. At the same time, 2017 was the year with the highest heat waves in Türkiye (Erlat et al. 2021).

In the SPI_3 maps for the month of July (-4.70 to -1.03), the normal drought values seen in the southern part in June (-5.96 to -1.02) are seen to increase in drought severity from southwest to north (Fig. 15). In the $SPEI_3$ index, the drought values that intensified in the eastern parts in June and July in 2021 are related to the effect of decreasing precipitation compared to normal and increasing temperature evaporation intensity (Taskın et al. 2022). RDI_3 drought severity in June (-5.24 to -1.28) and July (-4.15 to -1.06) is high in the inland and southeastern parts. In $SPEI_3$ June (-3.33 to -0.64) and July (-4.05 to -0.10), drought intensity increased at stations in the east of the study area (Fig. 15). In August, the effects of 2007–2008 drought intensity are observed in SPI_3 and $SPEI_3$ indices (Fig. 15). The fact that the drought intensified during the 2007–2008 periods is predominantly concentrated in the western, southern and eastern parts of the study area is related to the above-average temperature values in response to the decreasing precipitation values during this period (Simsek and Cakmak 2010; Türkes 2020b; Erlat and Güler 2023).

Similar to April, wet conditions in May are also high in 2013. In $SPEI_3$ (2.90), it was determined that the wet conditions increased in the northern part of Central Anatolia in 2022. In June, as in other months in 2013, RDI_3 (6.06) and SPI_3 (4.82) show an increase in wet conditions in the northwestern part. In the $SPEI_3$ (2.97) method, wet conditions are higher in the northeastern part of Central Anatolia in 2022. In $SPEI_3$ (3.03) and RDI_3 (5.72) for July in 2022, the highest values were found in the stations in the eastern areas. In SPI_3 (4.03), there is a high relative wet conditions in the east of the study area in 2015. In August, similar to July, increasing wet conditions are observed in $SPEI_3$ and RDI_3 methods in 2022. The eastern part for RDI_3 (5.77) and the southwestern part for $SPEI_3$ (3.03) have the highest wet conditions. In SPI_3 (3.31), the highest wet conditions were determined in the eastern part in 2016.

The years and areas with the highest drought values in September, October, November and December are shown in Fig. 16. In the SPI_3 maps for September (between -4.97 and -1.15), while normal arid conditions are generally dominant in the study area, there is an increase in drought severity in some stations in the eastern part. The increased drought severity in the eastern part in the SPI_3 index coincides with the hottest fall season in 2022 (Fig. 16). In RDI_3 (-4.04 to -1.20), there are no stations with high drought intensity outside of normal conditions, while in $SPEI_3$ (-3.19 to -0.94), drought intensity is high in the western coastal areas (Fig. 16). In 2006, the drought intensity observed in April is remarkable in RDI_3 September and SPI_3 October. The atmospheric conditions affecting the occurrence of heat waves, which have intensified especially since 2005, cause south sector winds, which increases the severity of drought (Erlat and Türkeş, 2015). The 2007–2008 drought severity observed in August is also observed in September and October in the $SPEI_3$ index (Fig. 16).

$SPEI_3$ shows normal arid conditions in October (-3.52 to -0.51), November (-3.46 to -0.88) and December (-4.39 to -1.03), with higher drought severity in the stations in the western and eastern parts of the Black Sea coast, respectively (Fig. 16). In the RDI_3 index (-4.33 to -0.33), the drought intensity, which increases only in October in the south, is represented by normal dry conditions in the other months. In the $SPEI_3$ index, drought intensity values are high in the western stations in September, inland in October, eastern in November and along the western Black Sea coast in December (Fig. 16). In SPI_3 and $SPEI_3$ indices, the effect of the increasing drought severity in the winter months of 2011–2012 is observed in SPI_3 and RDI_3 indices in November and December in the eastern parts. It is seen that the effect of winter drought is high with the high pressure conditions prevailing in continental regions and the effect of decreasing precipitation. The years 2020, when annual average temperatures increased, and 2021, when the most severe drought was experienced, are seen in RDI_3 November and $SPEI_3$ December (Fig. 16).

In September, the highest wet conditions belong to $SPEI_3$ (2.67) and RDI_3 (5.09) methods in 2022, while SPI_3 (3.15) method has the highest wet conditions in 2009. In $SPEI_3$ and SPI_3 methods, stations with high wet conditions were determined in the Black Sea coastal area and in the eastern part of the Black Sea coast in RDI_3 method. In October, RDI_3 (5.28) method in 2022, SPI_3 (3.29) and $SPEI_3$ (2.73) methods in 2015, the highest wet conditions are present in the stations in the eastern part of the study area. In 2022, RDI_3 (6.03) method in the east of the study area and $SPEI_3$ (3.33) in the Black Sea coastal area have high wet conditions in November. In the SPI_3 (3,56) method, wet conditions increased in the south of the Marmara Sea in 2013. December wet conditions in RDI_3 (5,79) method are the highest in the east of the study area in 2022. In 2001, the wet conditions increased in $SPEI_3$ (2,64) in the south of the study area and SPI_3 (3,25) in the western part of the station.

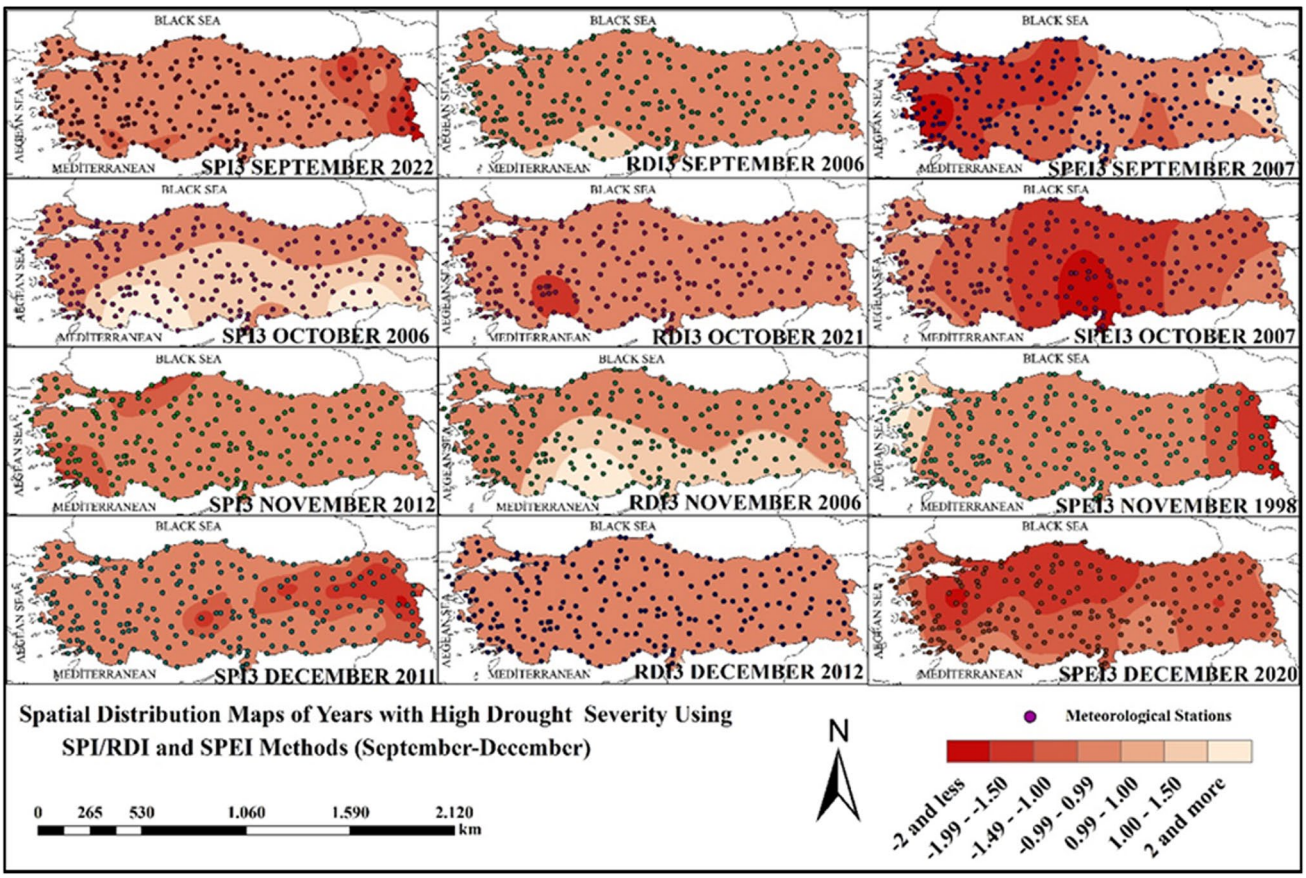

Fig. 16 Graphs of the years (September-December) in which the highest droughts were determined for each month of the 3-month analysis in SPI, SPEI and RDI methods

SPI, SPEI and RDI methods 6-month evaluation analyses

It provides seasonal precipitation forecasts by reflecting short- and medium-term wet conditions. Indices for 6, 9 and 12-month periods basically express medium and long-term trends in precipitation (WMO 2012). In the 6-month index results, the highest drought values were determined in 2011, 2012, 2013, 2014, 2016 and 2022 in the SPI method. In the RDI method, the highest drought values belong to the years 2006, 2007, 2012, 2013, 2017 and 2020. For the SPEI method, the years 1993, 2003, 2007, 2008, 2012, 2014, 2020 and 2021 are the years with the highest drought values. These years were mapped and the driest/wettest year and stations for each month are briefly summarized below.

The years and areas with the highest drought values in January, February, March and April are shown in Fig. 17. In the SPI_6 maps for January (-5.61 to -0.78), February (-5.94 to -0.96) and March (-5.28 to -0.85), it is seen that drought severity increases in the east of the study area (Fig. 17). The severe drought observed in January 2011 in $SPEI_3$ index is also observed in January in SPI_6 index. This shows that the effect of the decrease in winter precipitation seen in the 3-month analysis is also noticeable in the 6-month analysis (Fig. 17). Similar to the SPI_3 indices, the drought, which intensified in the eastern part of the country where the continental climate is observed in winter, continues to affect SPI_6 in February and March. In the April SPI_6 maps (between -5.32 and -1.04), high drought values are observed in the stations in the northeastern part of the study area (Fig. 17). In RDI_6 index, it was determined that the normal drought severity in January (-5.70 to -0.92) in the whole study area increased in February (-4.74 to -1.10) in the inland areas. The RDI_6 index was higher in March (-4.97 to -1.15) at the stations in the northern and western parts of the study area and in April (-5.40 to -1.07) at the stations in the east (Fig. 17). During these periods, topographic conditions and the effect of decreasing precipitation conditions cause an increasing effect on drought severity. In 2007, the period of severe drought was observed in March in RDI_6. The most severe drought period of 2013–2014 also shows its effect on the 6-month indices (Fig. 17).

SPI_6 April, RDI_6 January and SPI_6 indices show severe dry periods from February to April. These periods support

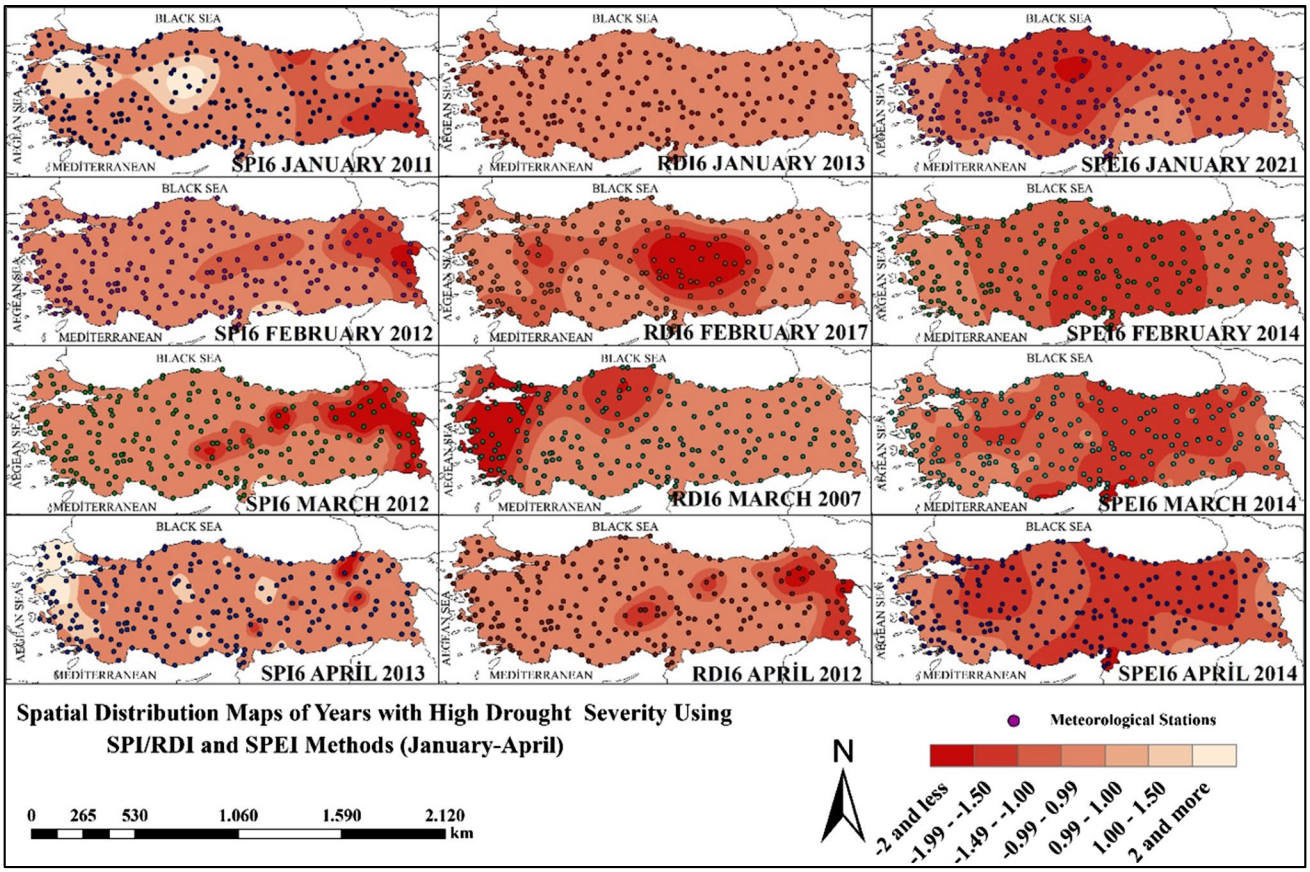

Fig. 17 Graphs of the years (January-April) in which the highest droughts were determined for each month of the 6-month analysis in SPI, SPEI and RDI methods

the yield decreases in agricultural products expressed in other studies (Akbas 2014; Taskın et al. 2022). In the maps prepared for the $SPEI_6$ index, drought severity increases from the north to the interior in January (between -3.01 and -0.88) and February (between -2.84 and -1.00). In March (-2.96 to -0.96) and April (-2.81 to -0.94), it is observed that it is effective from north to south in the eastern part of the study area (Fig. 17). The year 2021, when extreme drought was experienced, draws attention with its high drought severity in the $SPEI_6$ index throughout the study area (Erlat and Güler 2023).

The highest wet conditions in 2015 are observed in all three methods in the 6-month analysis in January. The highest wet conditions in RDI_6 (4.03) and SPI_6 (3.47) are in the southern part of the Marmara Sea. In $SPEI_6$ (2.64), the highest wet conditions is observed in Central Anatolia. In February 2015, similar to January, RDI6 (4.06) and SPI_6 (3.48) have high wet conditions in the southern part of the Marmara Sea. In $SPEI_6$ (2.60) method, the highest wet conditions in 2009 were highest in Central Anatolia. The highest wet conditions for March belongs to the Western Black Sea in 2022 for the RDI_6 (4.35) method. In 2019, SPI_6 (3.40) method had the highest wet in the southeast, while $SPEI_6$ (3.23) method had the highest wet conditions in the northern part of the Marmara Sea in 1998. In April 2013, SPI_6 (4.56) and RDI_6 (4.89) methods determined the highest wet conditions in the northwest of the study area. In the $SPEI_6$ (2.82) method, 2022 has the highest wet conditions in the Black Sea coastal area.

The years and areas with the highest drought values in May, June, July and August are shown in Fig. 18. It is seen that the drought values of the three index types in Türkiye increased between 2000 and 2014 with the effect of the record air temperatures observed between these years (Fig. 18). SPI_6 increases in the north–south direction in the east of the study area in May (-5.61 to -1.09), June (-5.39 to -1.20) and July (-5.92 to -1.05) (Fig. 18). In August (-4.77 to -1.03), there are high drought values in the southeastern part of the study area in SPI_6 index. In RDI_6 months, drought intensity increased from May (-5.64 to -1.07) to August (-5.29 to -1.11) in the western Black Sea coastal area (Fig. 18). In the $SPEI_6$ monthly $SPEI_6$ maps, the drought intensity increased only in the easternmost part of the study area in May (-3.44 to -0.90) and was replaced by normal

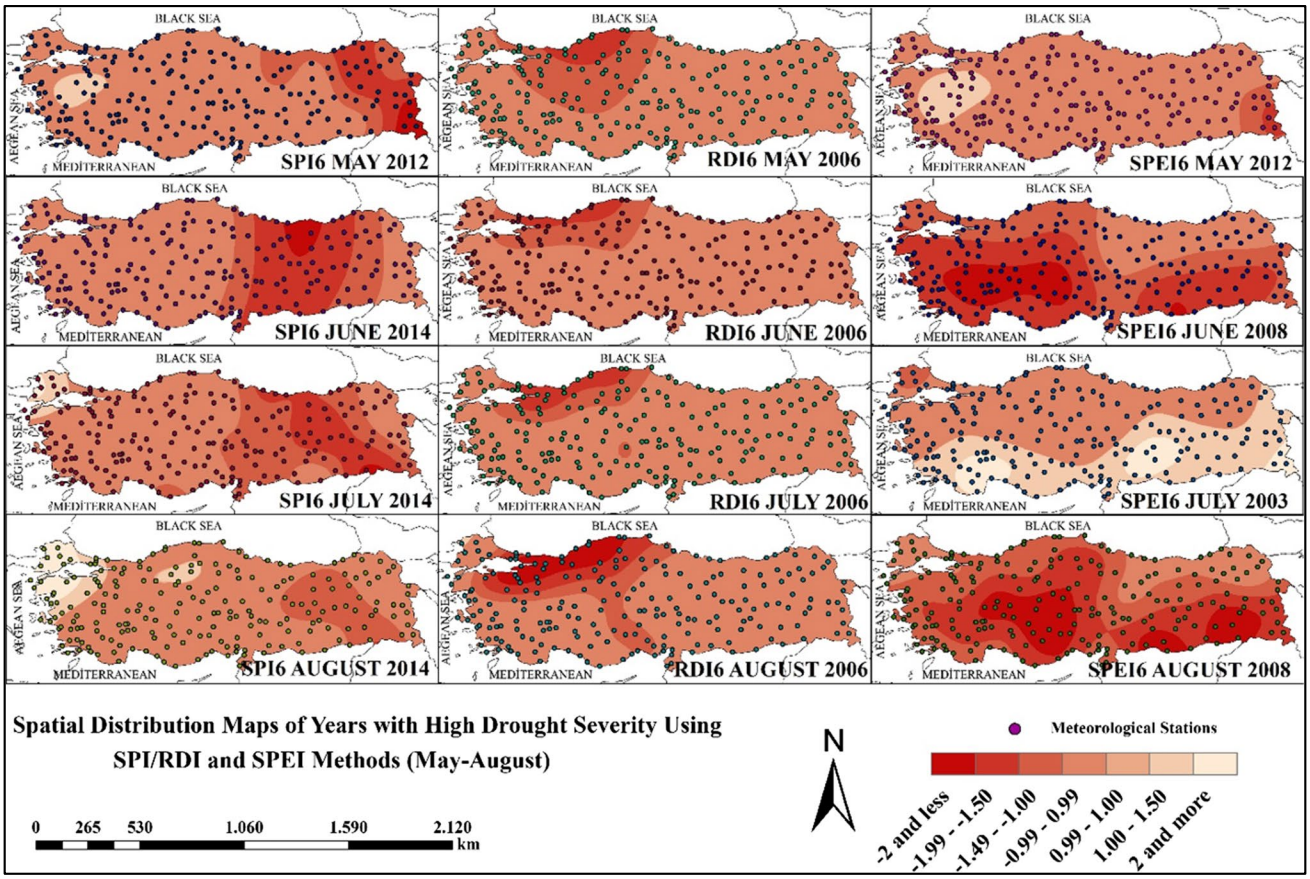

Fig. 18 Graphs of the years (May–August) in which the highest droughts were determined for each month of the 6-month analysis in SPI, SPEI and RDI methods

dry conditions in July (-3.26 to -0.35), moving from west to east (Fig. 18). The $SPEI_6$ maps for June (-3.27 to -0.88) and August (-3.94 to -0.50) similarly show a general increase in drought severity from west to southeast (Fig. 18). In 2012, the impact of high droughts is evident in SPI_6 and $SPEI_6$ in May. In 2014, severe drought with severe agricultural yield losses is observed in the eastern part between July and August in the SPI_6 index. The 2007–2008 $SPEI_6$, another period of severe drought and agricultural yield decline, was observed throughout the study area in July and August. While the yield decrease in wheat, which is an important food for the world, was 14% in 2008, this yield decrease was recorded as 13.8% in 2014 (Taskın et al. 2022). In the RDI_6 index, drought severity increased in the Western Black Sea coasts with increasing temperature values between May–November 2006.

Similar to April, in 2013, RDI_6 (5.86) and SPI_6 (5.28) methods show high wet conditions in the northwest of the study area. $SPEI_6$ (3.18) also shows high wet conditions on the south coast of the Marmara Sea in 2022. In June 2013, the highest wet conditions in RDI_6 (5.99) and SPI_6 (5.54) methods are the highest in similar areas with April and May. $SPEI_6$ (2.83) determined the highest wet conditions on the north coast of the Marmara Sea in 2022 as in other months. The high wet conditions observed in the northwest of the study area since April 2013 also belong to RDI_6 (6.01) and SPI_6 (5.20) methods in July. Similarly, the $SPEI_6$ (2.85) method shows the highest wet conditions in 2022, with high values in the western part. In August 2013, high wet conditions recur in the southwest of the study area in the RDI_6 (5.86) and SPI_6 (5.03) methods. In 2022, $SPEI_6$ (2.93) shows high wet conditions in the western Black Sea coastal area.

The years and areas with the highest drought values in September, October, November and December are shown in Fig. 19. In September, SPI_6 (-5.42 to -0.52) and $SPEI_6$ (-4.47 to -0.80) indices show high drought severity in the southwestern and southeastern parts of the study area, while RDI_6 (-5.22 to -1.33) shows high values in the western Black Sea region (Fig. 19). SPI_6 shows high drought intensity in the west, east and south in October (-5.66 to -0.93), expanding its area of influence in November (-5.74 to -0.84), while in December (-6.07 to -1.02) it is only observed at stations in the northeast (Fig. 19). RDI_6 October (-5.04 to -0.94) is characterized by high drought intensity in the western Black

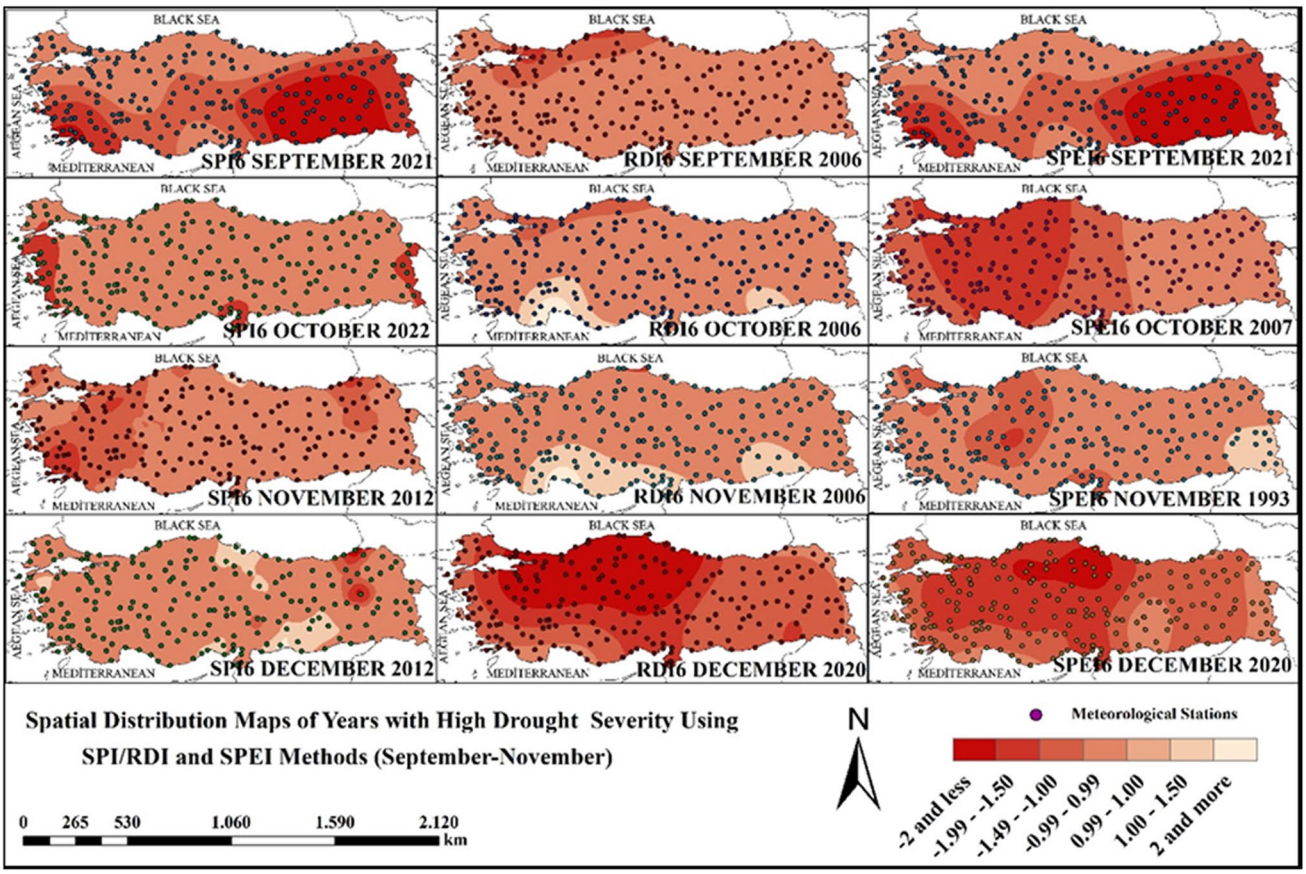

Fig. 19 Graphs of the years (September-December) in which the highest droughts were determined for each month of the 6-month analysis in SPI, SPEI and RDI methods

Sea region, while RDI_6 (-5.53 to -0.94) and $SPEI_6$ (-3.17 to -0.70) have normal dry conditions in November. In $SPEI_6$ October (-4.12 to -1.01) and December RDI_6 (-6.07 to -1.02) and $SPEI_6$ (-2.92 to -0.77) indices, drought intensity was high in the western parts and the area of influence expanded (Fig. 19). In 2012, drought severity increased in November and December in SPI_6 index (Fig. 19). However, while the increasing drought intensity in 2020 is in the west of the study area in $SPEI_6$ and RDI_6 indices, the drought intensity in 2021 is high in the west of the study area in September in SPI_6 and $SPEI_6$ indices. It is thought that the increasing temperatures in the winter season in 2020 may increase the evaporation intensity and cause an increase in drought severity in the western part (Fig. 19). In 2021, severe drought in the eastern part of the study area indicates that the effect of decreasing precipitation throughout the study area has increased in semi-arid areas such as the continental climate zone (Fig. 19).

In the September assessments, RDI_6 (5.68) and SPI_6 (4.72) have the highest wet conditions in 2013 in the northwest of the study area. The highest wet conditions in 2022 with SPEI6 (2.90) value is in the Mediterranean coastal area. The highest wet conditions in October is in the east of the study area with RDI_6 (6.16) in 2022 and SPI_6 (4.32) in 2015. In $SPEI_6$ (2.91) method, the highest wet conditions were determined in the Black Sea coastal area in 2022. The highest wet conditions in November in 2022 was in the east of the study area in RDI_6 (6.17) and in the Black Sea coastal area in SPEI6 (2.73). In SPI_6 (3.44) method, the highest wet conditions were determined in the south of the Marmara Sea in 2013. The highest wet conditions in December belong to the east of the study area in RDI_6 (6.23) and the Black Sea coastal area in $SPEI_6$ (2.77) in 2022. SPI_6 (3.20) in the Mediterranean coastal area has the highest wet conditions in 2001.

SPI, SPEI and RDI methods 9-month evaluation analyses

In drought indices, the driest/wettest years and stations were evaluated by months. In the SPI_9 method, 2007, 2012, 2013 and 2014, and in the RDI_9 method, 2006, 2007 and 2014 were the years with the highest drought values. In the $SPEI_9$ method, the highest drought values were determined

in 1994, 2003, 2007, 2014 and 2021. The months of these years were mapped and the spatial distribution of drought was shown.

The years and areas with the highest drought values in January, February, March and April are shown in Fig. 20. The effect of record temperatures between 2000 and 2014 caused an increase in drought severity in the 9-month index maps (Fig. 20). Especially after 1980, the Siberian anticyclone weakened and the Azores anticyclone became effective in the eastern Mediterranean, which led to an increase in winter drought (Topcu 2022). This would increase the impact of the North Atlantic Oscillation and lead to more recurrence of severe dry periods in Türkiye (Türkes 2020a; Topcu 2022). In the SPI_9 maps for January (-5.50 to -0.98) and February (-4.56 to -0.96), it was determined that normal dry conditions prevailed in general, although high drought values were observed at a few stations in the interior. SPI_9 The drought increase in January and February 2013, which was effective throughout the study area, caused a decrease in agricultural production. It affected cereal production and especially hazelnut production in the Black Sea region (Yılmaz 2023). The SPI_9 index shows a widening of the area of influence of drought severity in March, while high drought values are observed in April (between -4.96 and -0.83) in the eastern and inland areas (Fig. 20). It was determined that drought severity in 2012 increased in these continental climate areas due to the effect of decreasing precipitation due to topographic conditions in SPI_9 April.

In RDI_9 values, drought severity is high in January (-5.86 to -0.99), February (-5.87 to -1.04) and March (-5.77 to -0.91) in the coastal area from the western Black Sea to the south (Fig. 20). The fact that the highest drought in RDI_9 monthly indices between January-April 2007 was observed in the western coasts is related to the increased effect of the North Atlantic oscillation in this year (Türkes 2020b). As seen in Fig. 20, the effect of severe drought in 2014 is remarkable for the entire study area. In 2014, the increasing temperature-evaporation trend combined with decreasing precipitation was effective in the severity of drought between January and April, especially in $SPEI_9$ months. Drought intensity extending from north to south to coastal areas is observed in $SPEI_9$ January (between -3.15 and -1.04). Apart from these assessments, drought intensity is high from inland to eastward in $SPEI_9$ February (-2.92 to

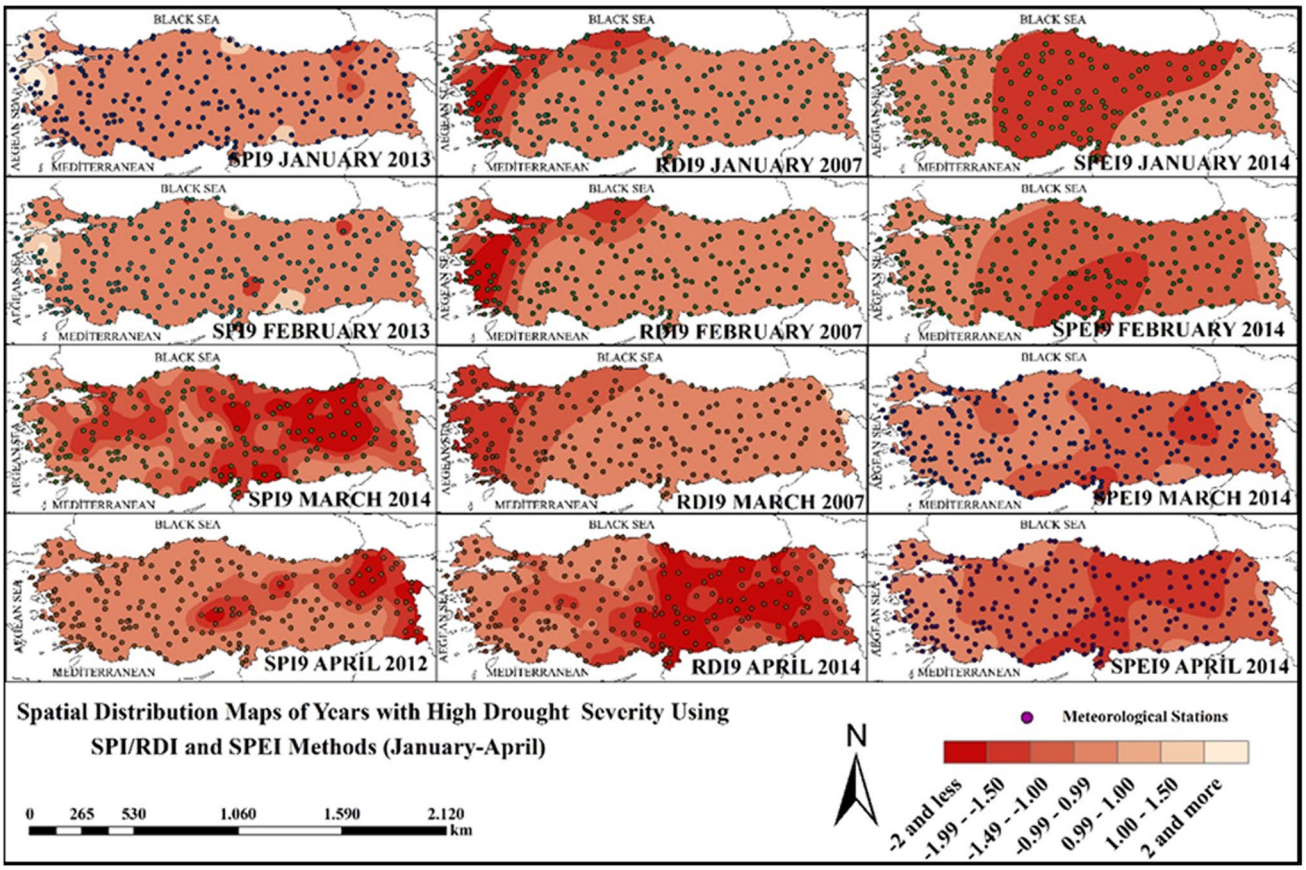

Fig. 20 Graphs of the years (January-April) in which the highest droughts were determined according to each month of the 9-month analysis in SPI, SPEI and RDI methods

-0.64), March (-3.08 to -0.78) and April (-3.00 to -0.79) and RDI_9 April (-5.52 to -0.74) (Fig. 20).

The highest wet conditions in January, February and March were in the southern part of the Marmara Sea in 2015.In RDI_9 method, the highest wet conditions were determined in January (4.48), February (4.30) and March (3.88). In SPI_9 method, the highest wet conditions were determined in January (3.98) and February (3.61) in the southern part of the Marmara Sea in 2015.The highest wet conditions in February $SPEI_9$ (2.63) were in Central Anatolia in 2019. In March, SPI_9 (3.30) in 2013 in the southeast and $SPEI_9$ (2.58) in 2022 in the Black Sea coast. In 2013, the highest wet conditions for April, RDI_9 (4.59) and SPI_9 (4.02) were in the northwest of the study area.In $SPEI_9$ (2.73) method, wet conditions show an increase in Central Anatolia in 2009.

The years and areas with the highest drought values in May, June, July and August are shown in Fig. 21. In SPI_9, the drought intensity increases from the western coastal areas towards the central Anatolia in May (-5.97 to -0.71), June (-5.80 to -0.82) and August (-5.84 to -1.06), and in July it is observed only in the northeastern coastal area (Fig. 21). In RDI_9 maps, unlike SPI_9, drought intensity increases towards the east of the study area in May (-5.51 to -0.90), June (-6.09 to -0.92) and July (-5.87 to -0.97) (Fig. 21). $SPEI_9$ drought intensity spread over the entire study area, centered in Central Anatolia in May (-3.03 to -0.83) and was high in the northern and western parts in June (-3.75 to -0.85) and July (-2.84 to -0.86) (Fig. 21). $SPEI_9$ August (-3.17 to -1.02) is dominated by normal drought values. The 2007 drought intensity, which is effective in SPI_9 May, June, August and $SPEI_9$ July, is observed in the western part (Fig. 21). Consistent with the other indices, the effect of the North Atlantic Oscillation led to an increase in summer drought. In 2014, the severe drought effect was determined to be severe in the eastern part between RDI_9 May–July. The effect of 2021, another severe drought year, is prominent throughout the study area in $SPEI_9$ May with increasing temperature and evaporation (Fig. 21).

May wet conditions in RDI_9 (5.50) and SPI_9 (4.84) indices are the highest in 2013 in the northwestern part. An increase is observed in $SPEI_9$ (2.77) values in the West Black Sea coastal region in 2022. Similarly, in June, it was determined that the increase in wet conditions continued in the northwest station in RDI_9 (5.50) and SPI_9 (4.99) indices in

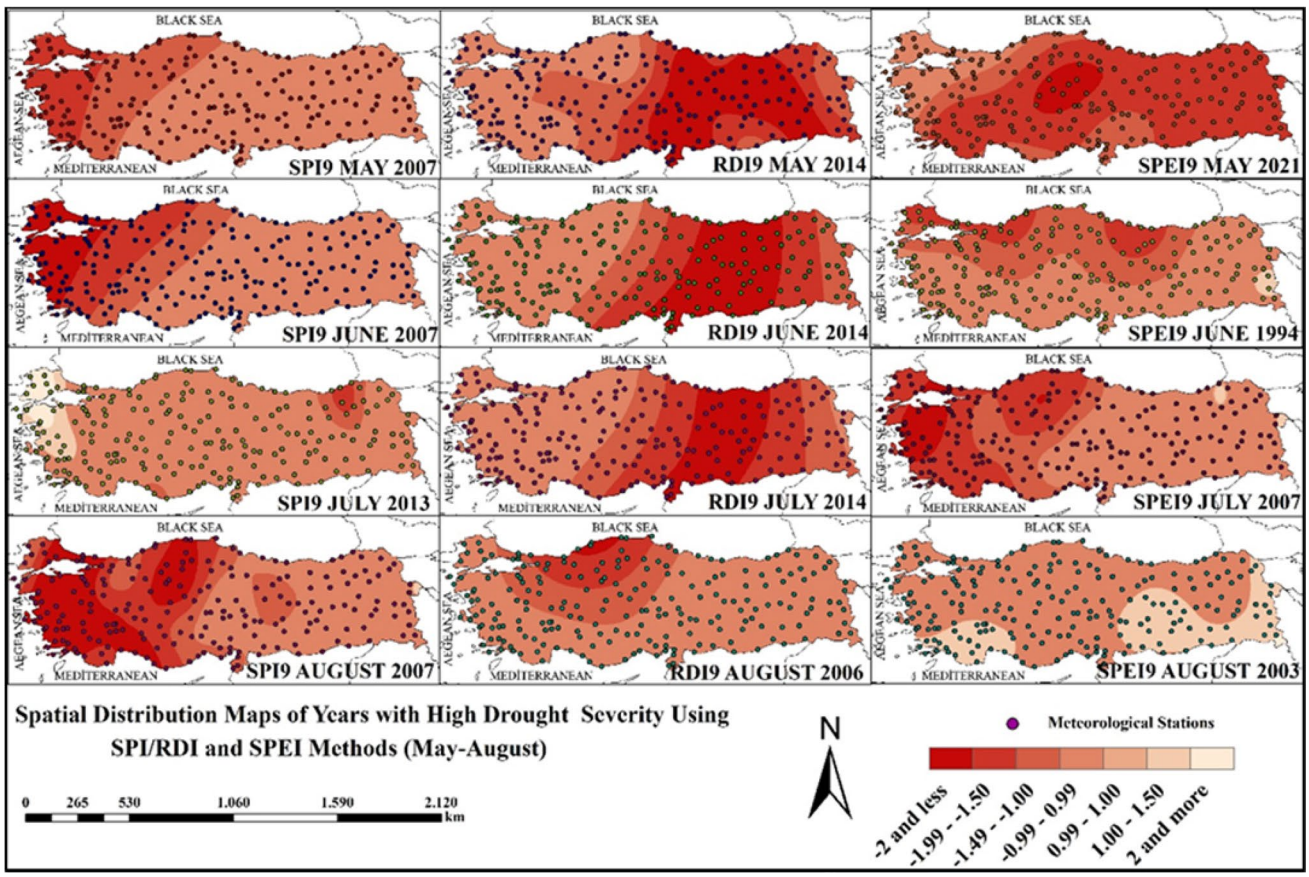

Fig. 21 Graphs of the years (May–August) in which the highest droughts were determined for each month of the 9-month analysis in SPI, SPEI and RDI methods

2013. $SPEI_9$ (2,92) has the highest wet conditions in the northern part of the Marmara Sea in 1998. It is observed that the wet conditions increased in 2013 in the northwest of the study area in July. RDI_9 (5,60), SPI_9 (5,05) and $SPEI_9$ (2,95) wet conditions increased in 2022. In August, RDI_9 (5.72), SPI_9 (4.92) in the northwest in 2022 and $SPEI_9$ (3.56) in the south of the Marmara Sea with the highest wet conditions.

The years and areas with the highest drought values in September, October, November and December are shown in Fig. 22. The SPI_9 is higher in the east and south inland in November, extending from north to south in the east of the study area in September (-5.54 to -1.30). Normal dry conditions are present in October (-6.00 to -0.87) and November (-4.46 to -0.94) (Fig. 22). SPI_9 September–November is characterized by the impact of the 2014 severe drought, while November and December are characterized by the 2012 severe drought in the eastern part (Fig. 22). RDI_9 in September (-5.77 to -1.31), the effect of the increasing drought severity in the western Black Sea coastal area continues until December (-5.83 to -1.12). In addition, drought intensity increases in the coastal area from the Western Black Sea to the south in December (Fig. 22). In the RDI_9 index, the severe drought that was effective in the northern coastal region from August to December 2006 caused an increase in the drought effect of the lack of precipitation, especially in winter months (Partal and Yavuz 2020).

Normal dry conditions in the study area give way to high drought values in the north in September $SPEI_9$ (-3.82 to -0.82) (Fig. 22). In October (-3.34 to -0.71), drought intensity is also high in the western part, while in November (-3.12 to -0.70) and December (-3.82 to -1.07), drought intensity increases from the southeast (Fig. 22). In 2021, it is observed that drought severity increased in November–December in the $SPEI_9$ index with low precipitation at normal precipitation values and increasing temperature evaporation values in the southern part (Fig. 22).

The highest wet conditions with the values determined in RDI_9 (5.57) and SPI_9 (4.78) indices in September are in the northwestern part of the study area in 2013. With the value of $SPEI_9$ (3.20), wet conditions increase in the south of Marmara in 2022. In the northwest of the study area, there is high wet in RDI_9 (5.50) and SPI_9 (4.74) methods in October 2013. The highest wet with SPEI9 (2.94) value is in the south of Marmara in 2022. In November 2022, RDI_9 (5.34) in the western Black Sea coastal area and $SPEI_9$ (2.95) in the eastern part of the study area have increased wet conditions.

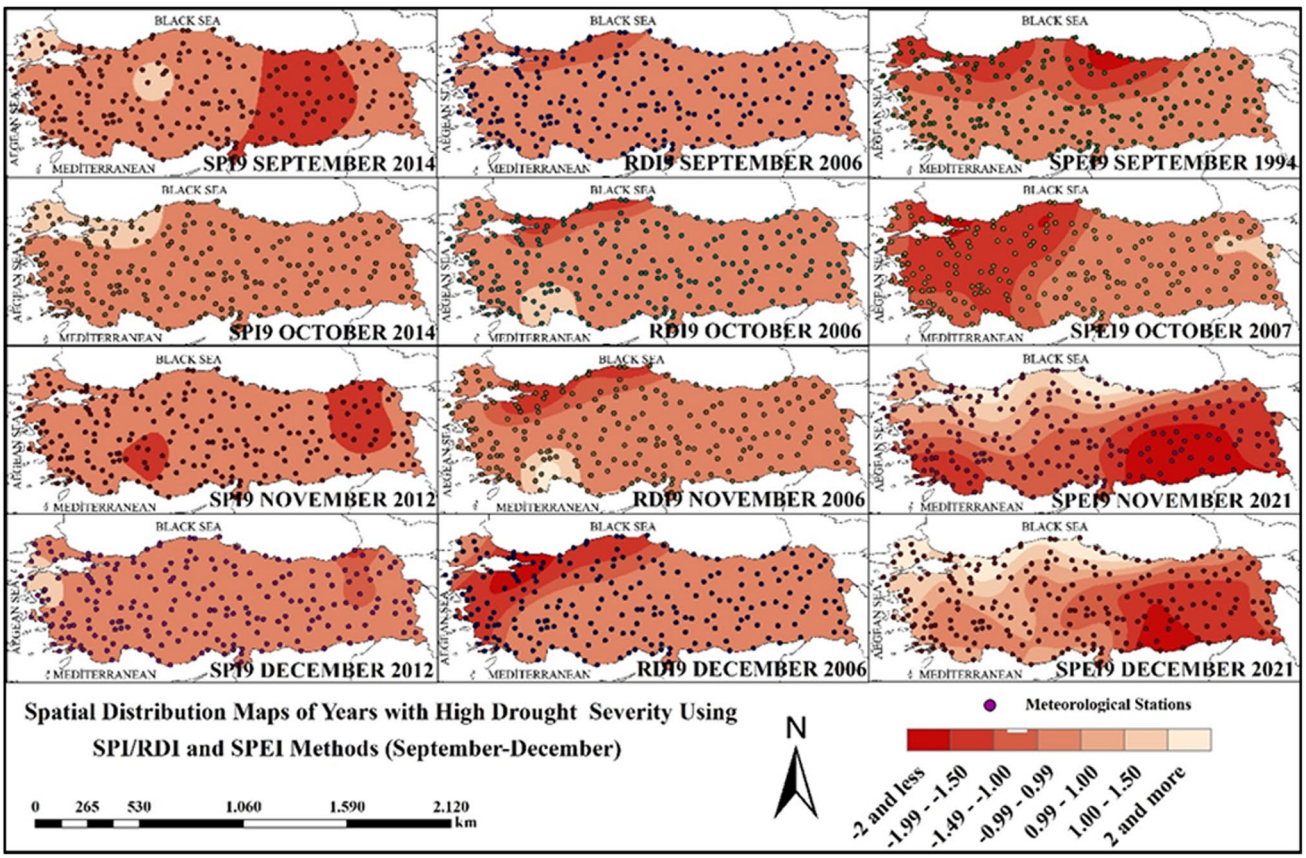

Fig. 22 Graphs of the years (September-December) in which the highest droughts were determined by each month of the 9-month analysis in SPI, SPEI and RDI methods

For SPI_9 (4.66), high wet conditions were determined in the northwestern part of the study area in 2013. In December 2022, RDI_9 (5,12) in the western Black Sea coastal area and $SPEI_9$ (2,73) in the north of the study area, and SPI_9 (4,30) in the northwestern part of the study area in 2013, wet conditions increase.

SPI, SPEI and RDI methods 12-month evaluation analyses

In the 12-month analyses where long-term drought is expressed, the highest drought values were determined in 2006, 2007, 2012, 2013 and 2014 in the SPI method and in 2006, 2007, 2013 and 2014 in the RDI method. In SPEI management, the highest drought values are found in 1994, 2008, 2012, 2014 and 2015. By mapping the months of these years, the spatial distribution of drought is visually presented.

The years and areas with the highest drought values in January, February, March and April are shown in Fig. 23. It is seen that the year 2014, which was a severe drought year for Türkiye, caused high drought severity in March and April across the study area in SPI_{12}/RDI_{12} and $SPEI_{12}$ indices (Fig. 23). In the SPI_{12} maps, the area of influence of drought severity is large in January (-5.15 to -0.98), March (-4.42 to -0.88) and April (-5.20 to -0.85) (Fig. 23). In February (-5.40 to -0.86), drought intensity increased in the northeastern coastal area. RDI_{12} showed high drought intensity in January (-6.16 to -0.94) and February (-6.03 to -1.10) in the west coast and western Black Sea, while in March (-6.40 to -0.97), increased drought values were determined in the northeast and a few stations in the south (Fig. 23). Similar to SPI_{12}, drought intensity was high throughout the study area in RDI_{12}. $SPEI_{12}$ increased in January (-3.21 to -0.71), March (-2.96 to -0.87) and April (-3.06 to -0.99), extending southward along the eastern Black Sea coast, and increased in February (-3.35 to -0.81) in the western part (Fig. 23). In January SPI_{12} and $SPEI_{12}$, the severe drought values of 2014 are also noteworthy. The increased agricultural loss due to the winter drought in this period and the frost in March support the results of this study (Taskın et al. 2022). Since 2008, the severe drought in 2013 and 2014, which was affected by increasing temperature and decreasing precipitation, became evident in March RDI_{12} and February SPI_{12} (Fig. 23). Another severe dry period and agricultural losses in 2007–2008

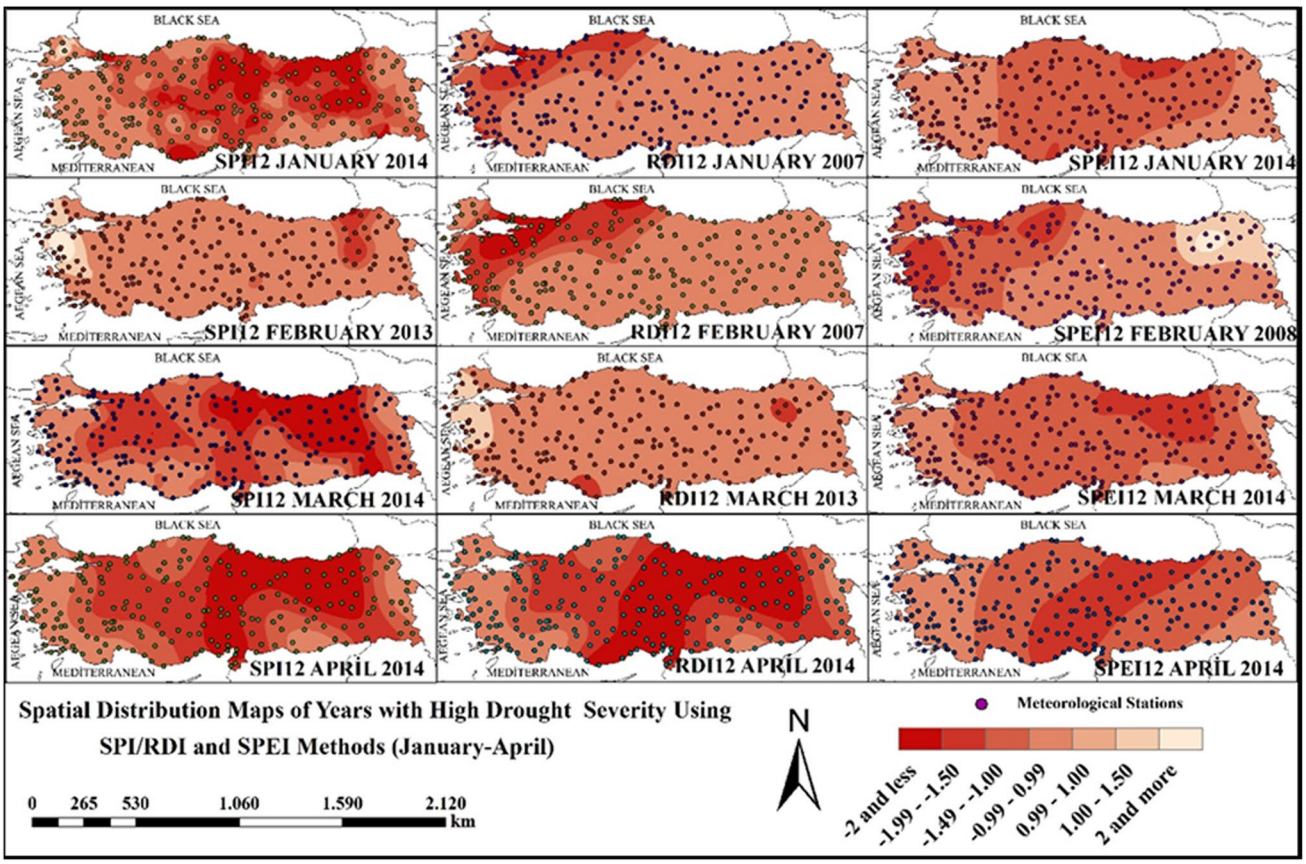

Fig. 23 Graphs of the years (January-April) in which the highest droughts were determined for each month of the 12-month analysis in SPI, SPEI and RDI methods

were observed in January–February RDI_{12} and February SPI_{12} in the western part.

The highest January wet conditions for RDI_{12} (5.18) and SPI_{12} (4.52) were in 2014 in the northwest of the study area. For $SPEI_{12}$ (2.66), wet increased in the Black Sea coastal area in 2010, while the highest wet conditions were determined for RDI_{12} (4.92), SPI_{12} (4.25) and $SPIE_{12}$ (2.62) in 2014 in the northwest of the study area in February. In March, similar to the other months, RDI_{12} (4.86), SPI_{12} (4.10) and $SPEI_{12}$ (2.66) had the highest wet conditions in the northwest of the study area in 2014. In April, similar to the other months in 2013, RDI12 (4.13) in the northwest has the highest wet conditions. SPI_{12} (3.72) in Central Anatolia in 2015 and $SPEI_{12}$ (3.15) in 2019 have the highest wet conditions in the southeast.

The years and areas with the highest drought values in May, June, July and August are shown in Fig. 24. SPI_{12} shows high drought severity on the west coast in May (-5.99 to -0.58), July (-5.76 to -0.77) and August (-5.94 to -0.76), while dry conditions prevail throughout the study area in July (Fig. 24). RDI_{12} monthly assessments show high drought intensity in the east of the study area from May (-5.56 to -0.82) to August (-6.07 to -1.11). In $SPEI_{12}$ May (-2.94 to -0.72), June (-2.93 to -0.78) and July (-2.88 to -0.92), drought intensity was high in the east of the study area and increased in August (-3.24 to -0.86) in the northern part (Fig. 24). While the severe drought values of the 2006–2007 period were high in the western part of the study area in SPI_{12} May–August, it is seen that the effect of drought severity in 2014 increased in the continental climate zone in the eastern part of the study area in RDI_{12} and $SPEI_{12}$ indices (Fig. 24).

The highest wet conditions for May belong to RDI_{12} (5.18), SPI_{12} (4.57), and $SPEI_{12}$ (2.70) indices in 2013. Similar to May, wet increases in the northwest of the study area in RDI_{12} (5.38) and SPI_{12} (4.64) methods in 2013. The Eastern Black Sea coastal area has the highest wet conditions determined by the $SPEI_{12}$ (2.81) method in 2022. Similar to June, $SPEI_{12}$ (2.94) value is high in the Eastern Black Sea coastal area in 2022. RDI_{12} (5.36) and SPI_{12} (4.65) methods show high wet conditions for the northwest of the study area in 2013. In $SPEI_{12}$ (3.00) method, wet conditions increase in the northern part of the Marmara Sea in 2022.

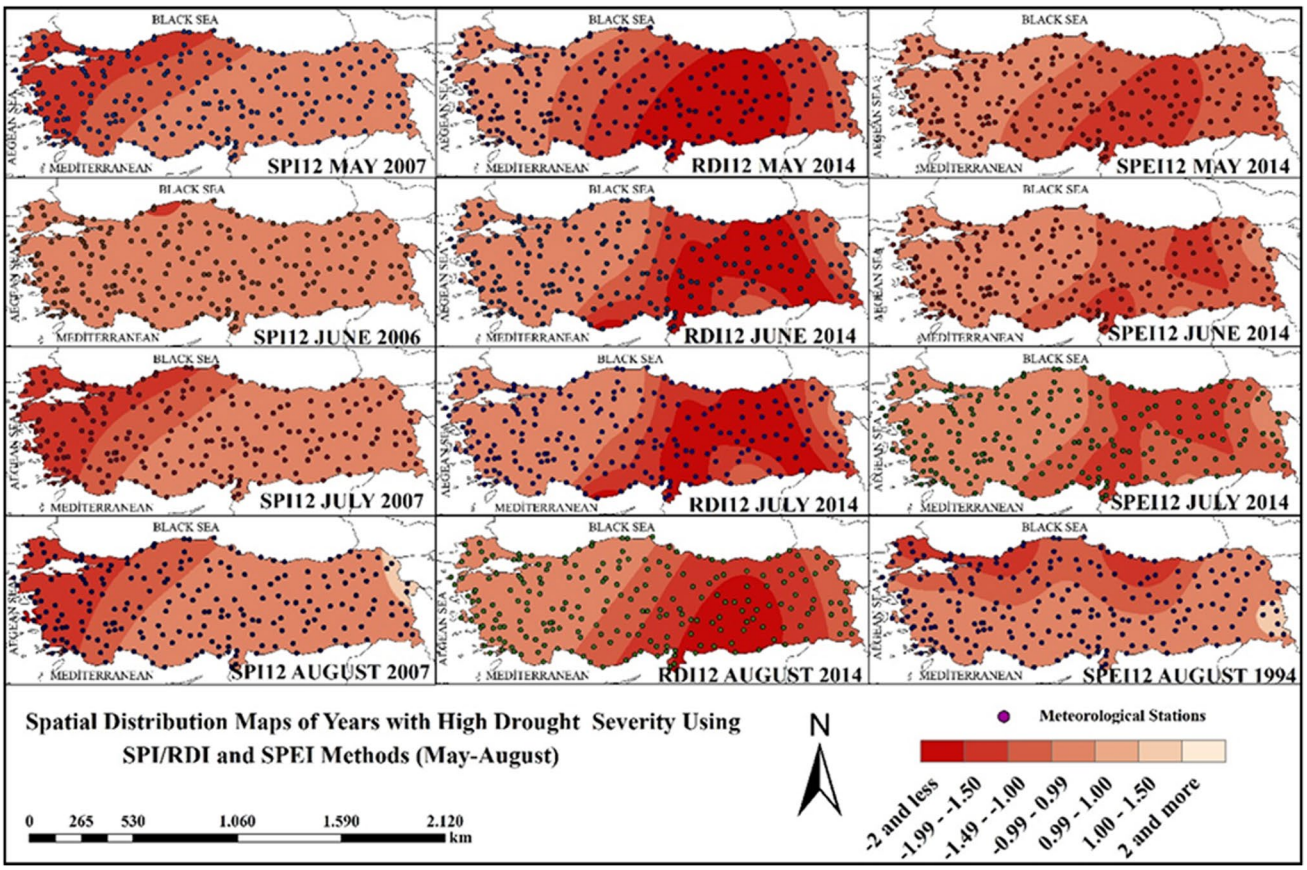

Fig. 24 Graphs of the years (May–August) in which the highest droughts were determined for each month of the 12-month analysis in SPI, SPEI and RDI methods

The years and areas with the highest drought values in September, October, November and December are shown in Fig. 25. From September to December, there is an increasing drought severity in the eastern and coastal areas in SPI_{12} (-5.76 to -0.64) and in the western Black Sea coastal area in RDI_{12} (-5.84 to -1.09) (Fig. 25). In $SPEI_{12}$ maps, drought values are high in the northern part in September (-3.00 to -0.45), while normal drought values dominate in October (-2.69 to -0.49) and November (-3.07 to -0.66). In $SPEI_{12}$ December (-3.02 to -0.56), drought intensity was high in the west coast and southeast stations (Fig. 25). Drought severity increases in the east of the study area during the high drought periods of 2012–2013. This can be explained by both topographic conditions and decreasing precipitation due to the effect of increasing temperature in continental regions. This drought effect between September-December in SPI_{12} was effective in November in $SPEI_{12}$ (Fig. 25). In 2006, the drought effect intensified in the northern part of the region between September and December in RDI_{12} monthly. The effect of decreasing precipitation in this region causes the increase in drought severity in 2006 (Partal and Yavuz 2020). The increasing atmospheric temperature and heavy precipitation in the Black Sea region support the increasing drought severity (Donava 2017).

In September, RDI_{12} (5.16) and SPI_{12} (4.45) show the highest values in the northwestern part, while $SPEI_{12}$ (2.85) shows extremely humid values in the western Black Sea coastal region in 2022. October RDI_{12} (5.37) in 2022 shows an increase in extremely humid in the Western Black Sea coastal region and $SPEI_{12}$ (2.85) in Central Anatolia. SPI_{12} (4.62) values in 2013, indicating extremely humid conditions, are in the northwest of the study area. In November and December in 2022, RDI_{12} shows an increase in extremely humid in the western Black Sea coastal area and SPI_{12} in the northwest of the study area. For $SPEI_{12}$ in 2022, in November (3.41) Mediterranean coastal area and in December (2.91), extremely humid conditions prevail in the south of Central Anatolia.

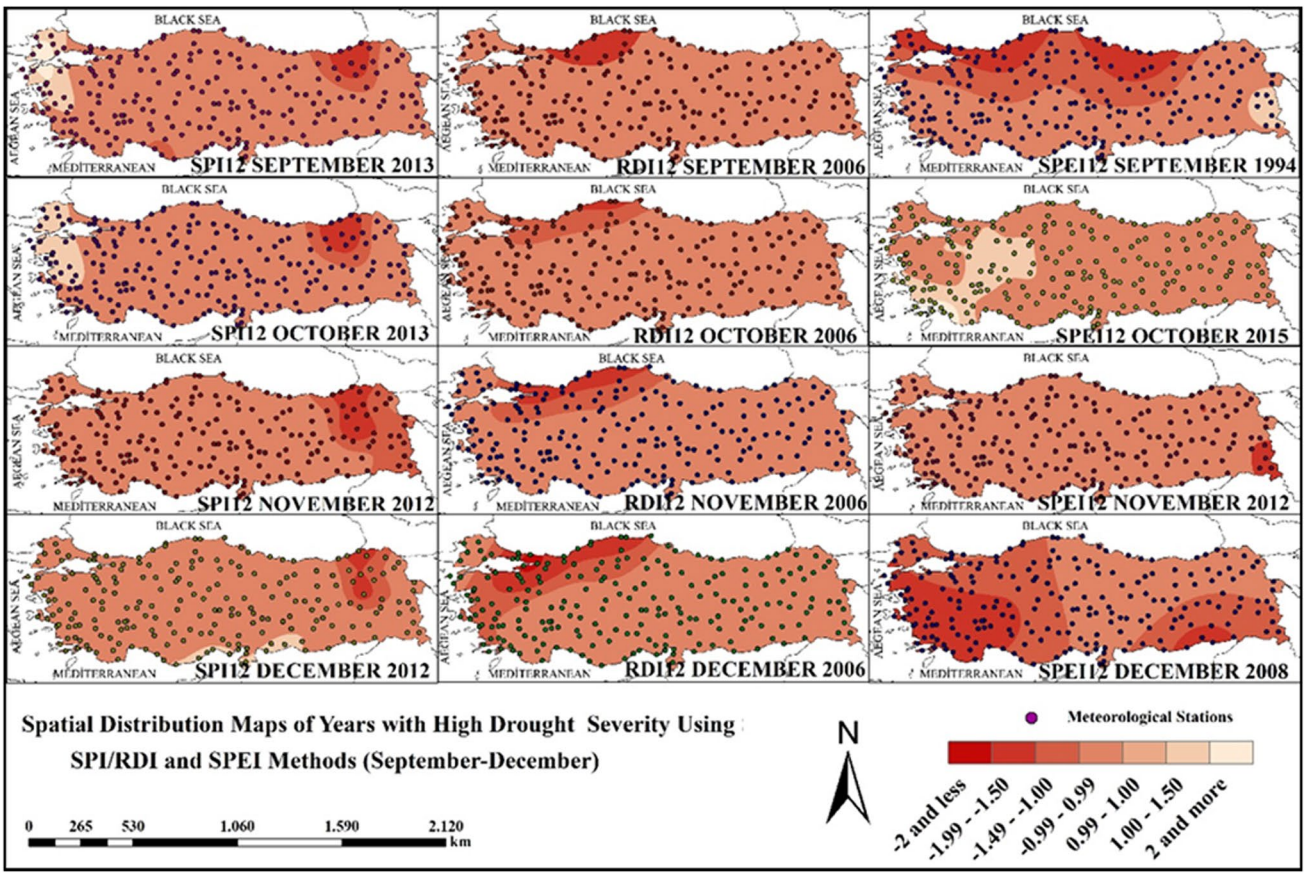

Fig. 25 Graphs of the years (September-December) in which the highest droughts were determined for each month of the 12-month analysis in SPI, SPEI and RDI methods

Conclusion and assessment

This study includes a comprehensive drought analysis for Türkiye covering the period 1991–2022. In this analysis, SPI, SPEI and RDI methods are used to present the spatial and temporal variation of drought, the impact of geographical factors on this variation and its agricultural consequences in detail. In the study area, meteorological drought events are experienced more frequently than in the past years due to the long-term below-normal precipitation and increasing temperature. In addition, Türkiye's topographic conditions and its location in the Mediterranean basin, which is a sensitive area to climate change, are among the most important factors affecting the temporal and spatial variation of the rule. The results of the study are given below:

- In the SPI, SPEI and RDI methods applied by using the data of 219 meteorological stations between 1991 and 2022 covering the study period, it was observed that the slightly arid class range (0.99 to -0.99) had the highest recurrence rate. One reason for Türkiye's tendency to shift to more arid conditions in the last 20 years is the increasing trend in annual average temperatures in the Mediterranean basin where Türkiye is located, increasing the frequency and duration of heat waves and the areas affected by them (Güler and Erlat 2023).
- Among the three indices SPI, SPEI and RDI, it is observed that drought severity generally increases in the whole study area. In short-term drought analyses, dry periods are more recurring, whereas in long-term analyses, dry periods are less recurring. One of the main reasons for this situation is the variability of precipitation periods from year to year and the increase in heavy rainfall due to increasing temperatures with global climate change. With the increase in temperature, atmospheric evaporation rates cause more intense and intense precipitation. Although this situation shows the absence of precipitation in short-term drought analyzes, it has a misleading effect. The most important feature of climate change is that wet periods are wetter and dry periods are more severe droughts. Especially in Türkiye, the increase in surface runoff with the effect of heavy precipitation from 2010–2021 increases the severity of drought by reducing the amount of water stored in the soil.
- In the 1-month indices, the seasonal variability of precipitation caused the areas where drought severity increased to differ according to the indices. Especially in the winter months, SPI, SPEI and RDI reflect the drought severity in the western coasts and in the whole study area, while SPI and RDI show the drought severity in the northern and eastern parts best in other months. In the SPEI index, drought variation is high in the eastern parts.
- In the 3-month indices, the SPI index draws attention to increased drought severity in the eastern and western parts, while the RDI index draws attention to increased drought severity in the northern parts. In SPEI indices, periodically changing drought severity is effective in the northern and western coastal and continental regions.
- In the 6-month indices, drought severity increases in the eastern parts for the SPI index. RDI 6-month indices show high drought severity in the northern coastal areas, while SPEI index type shows high drought severity in the western coasts and eastern parts.
- Although long-term severe drought varies periodically in the 9- and 12-month indices, it is observed that the stations in the northern and western coasts and in the eastern part have similarities in examined indexes.
- In the long-term drought indices, fewer but long-lasting dry periods are noteworthy. This situation is the result of the variability of the mid-latitude wandering depressions, which are among the atmospheric conditions that control the climate of Türkiye, according to the North Atlantic oscillation, and the year-to-year and seasonal changes in precipitation (Türkes 2020b). In periods when the North Atlantic oscillation is positive, especially the winter season is colder and less rainy. The relationship between the severe dry periods in Türkiye and the periods when the North Atlantic oscillation is positive, which is also included in the results of the study, has a wide place in the literature (Kömüscü, 2001; Tatlı and Türkes 2008; Türkes 2020b; Topcu 2022). Long-term droughts with high severity of heat waves and decreased precipitation have an impact on agricultural production (Sen et al. 2012; Ozelkan et al. 2016; Taskın et al. 2022).

This study can form a basis for building resilient and sustainable societies against climate change and drought. The future goal of this study, which was carried out in Türkiye, one of the regions where climate change is felt the most, is to reveal the effects of different types of drought (meteorological, hydrological, agricultural and socioeconomic) with quantitative and qualitative data obtained from field studies.

Author contributions Fatma Yaman Öz: analysis; research; data editing; visualization, writing-original draft; Emre Özelkan: theoretical background, organization review and editing, supervision. Hasan Tatlı: data acquisition, review and organization, supervision. There is no financial support in our study.

Funding Open access funding provided by the Scientific and Technological Research Council of Türkiye (TÜBİTAK).

Data Availability No datasets were generated or analysed during the current study.

Declarations

Disclosure statement No potential conflict of interest was reported by the authors.

Financing statement There is no financial support for the preparation of the article.

Competing interests The authors declare no competing interests.

References

Abbes A, Inoubli R, Rhif M, Farah İ (2023) Combining deep learning methods and multi-resolution analysis for drought forecasting modeling. Earth Sci Inf 16(2):1811–1820

Akbas A (2014) Distribution of climatological drought probabilities in Turkey. Journal of Turkish Geography (63):1–7. https://doi.org/10.17211/tcd.08368

Akhtari R, Morid S, Mahdian MH, Smakhtin Vladimir (2009) Assessment of areal interpolation methods for spatial analysis of SPI and EDI drought indices. Int J Climatol 29:135–145. https://doi.org/10.1002/joc.1691

Aksu HH (2023) Estimation and analysis of seasonal rainfall distribution and potential of Türkiye and its 25 main watersheds. Atmosphere 14(5):1–17. https://doi.org/10.3390/atmos14050800

Ali M, Younes K, Esmail A, Fatemeh T (2011) Assessment of geostatistical methods for spatial analysis of SPI and EDI drought indices. World Appl Sci J 15(2):474–482

Avcı M (2005) Flora of Turkey in terms of Diversity and Endemism. J Geogr 13:27–55

Aydın O (2014) Determination of Average Annual Total Precipitation in Turkey by Kriging Method. Ankara University Institute of Social Sciences, Ankara

Badji O, Zhu Y, Lü H, Guédé KG, Chen T, Oumarou A, ... Brice S (2023) The effects of drought in the Huaibei plain of China due to climate change. Atmosphere 14(860):1–19

Bahadır M (2013) Determination of spatial changes in Akşehir Lake by remote sensing techniques. Marmara J Geogr 28:246–275

Bakanogulları F (2020) Analysis of drought severity in Istanbul-Damlıca stream basin using SPEI and SPI indices. Soil Water J 1(9):1–10

Biswas A, Si B (2013) Model Averaging for Semivariogram Model Parameters. In: Grundas S, Stepniewski A (eds) Advances in Agrophysical Research. pp 82–95

Byun H, Wilhite H (1999) Objective quantification of drought severity and duration. J Clim 12:2747–2756

Caglıyan A, Ayhan G (2018) Spatial analysis of precipitation in Turkey. In: TUCAUM 30th Anniversary International Geography Symposium. Ankara, pp 103–120

Dai M, Huang S, Huang Q, Leng G, Guo Y, Wang L, ... Zheng X (2020) Assessing agricultural drought risk and its dynamic evolution characteristics. Agric Water Manag 231:1–12

Das J, Gayen A, Saha P, Bhattacharya S (2020) Meteorological drought analysis using Standardized Precipitation Index over Luni River Basin in Rajasthan, India. SN Appl Sci 2:1–17

De Martonne E (1926) Une nouvelle fanction climatologique: l'indice d'aridité. La Météorologie 2:449–458

Donava TE (2017) Variability of conditions for water phase transitions in the atmosphere of the Black Sea region. In: 23rd International Symposium on Atmospheric and Ocean Optics: Atmospheric Physics. https://doi.org/10.1117/12.2286848

Erlat E, Güler H (2023) Temporal variation of droughts according to Standardized Precipitation Evapotranspiration Index (SPEI) in Turkey (1951–2022). J Aegean Geogr 32:77–90. (100th Year of the Republic Special Issue)

Erlat E, Türkeş M (2015) Changes in the frequencies of record maximum and minimum air temperatures in Turkey during 1950–2014 and their relations with atmospheric conditions. J Aegean Geogr 24(2):29–55

Erlat E, Türkes M, Aydın-Kandemir F (2021) Observed changes and trends in heatwave characteristics in Turkey since 1950. Theoret Appl Climatol 145(1):137–157

Gocic M, Trajkovic S (2013) Analysis of precipitation and drought data in Serbia over the period 1980–2010. J Hydrol 494:32–42

Güler H, Erlat E (2023) Changes and trends in average air temperatures in Turkey during 1950–2022. J Aegean Geogr 32(1):1–17. https://doi.org/10.51800/ecd.1281319

Günal N (2013) Effects of climate on natural vegetation in Turkey. Acta Turcıca (Online Thematic Journal of Turkic Studies) (1):1–22. http://www.actaturcica.com/

Guo Y, Huang S, Huang Q, Leng G, Fang W, Wang L, Wang H (2020) Propagation thresholds of meteorological drought for triggering hydrological drought at various levels. Sci Total Environ 712:1–12

Hadi J, Tombul M (2018) Comparison of spatial interpolation methods of precipitation and temperature using multiple integration periods. J Indian Soc Remote Sens 46:1187–1199

Isaaks E, Srivastava R (1989) Applied Geostatistics. Oxford University Press, New York

Isia I, Hadibarata T, Jusoh M, Bhattacharjya R, Shahedan N, Bouaissi A, ... Syafrudin M (2023) Drought analysis based on standardized precipitation evapotranspiration index and standardized precipitation index in Sarawak, Malaysia. Sustainability 15:1–18

Jabbi F, Li Y, Zhang T, Bin W, Hassan W, Songcai Y (2021) Impacts of temperature trends and SPEI on yields of major cereal crops in the Gambia. Sustainability 13:1–19

Kale MM (2021) Hydrological drought analysis for Akarçay closed basin. J Geogr 42:165–180

Kapluhan E (2023) Drought and its effects on Turkish agriculture. Iksad Publications, Ankara

Khorrami B, Gündüz O (2019) Improved Spatial Variation Pattern for Monthly Average Precipitation Based on Geostatistical Interpolation Techniques A Case Study from Izmir-Turkey. In: 10th National Hydrology Congress. Muğla Sıtkı Koçman University, Muğla

Khorrami B, Gündüz O (2021) Quantitative analysis of surface interpolation techniques for estimation of long-term average total precipitation distribution for Turkey. In: 14th National 2nd International Environmental Engineering Congress (Conference Paper). TMMOB Chamber of Environmental Engineers

Kömüscü A, Turgu E, Deliberty T (2022) Dynamics of precipitation regions of Turkey: a clustering approach by K-means methodology in respect of climate variability. J Water Clim Change 13(10):1–29. https://doi.org/10.2166/wcc.2022.186

Kömüscü A (2001) An analysis of recent drought conditions in Turkey in relation to circulation patterns. Drought Network News 22

Lange M (2020) Climate Change in the Mediterranean: Environmental Impacts and Extreme Events. European Institute of the Mediterranean (IEMed). pp. 30–45

Lim Kam Sian K, Zhi X, Ayugi B, Onyutha C, Shilenje Z (2023) Meteorological drought variability over Africa from multisource datasets. Atmosphere 14(1052):1–25

Lionella P, Scarascia L (2018) The relation between climate change in the Mediterranean region and global warming. Reg Environ Change 18:1481–1493

Malik A, Kumar A (2021) Application of standardized precipitation index for monitoring meteorological drought and wet conditions in Garhwal region (Uttarakhand). Arab J Geosci 14(1):21

McKee TB, Doesken NJ, Kleist J (1993) The relationship of drought frequency and duration to time scale. Proceedings of the Eighth Conference on Applied Climatology, (s. 17–22). Anaheim, CA

Mehr A, Sorman A, Kahya E, Afshar M (2020) Climate change impacts on meteorological drought using SPI and SPEI: case study of Ankara, Turkey. Hydrol Sci J 65(2):254–268. https://doi.org/10.1080/02626667.2019.1691218

MGM (2022) Precipitation Assessment. . C. MINISTRY OF ENVIRONMENT, URBANIZATION AND CLIMATE CHANGE General Directorate of Meteorology, Ankara

MGM (2023) Precipitation Assessment. Araştırma Dairesi Başkanlığı Hidrometeoroloji Şube Müdürlüğü. T. C. Republic of Turkey Ministry of Environment, Urbanization and Climate Change General Directorate of Meteorology, Ankara

Miro JJ, Estrela MJ, Corell D, Gomez D, Luna MY (2023) Precipitation and drought trends (1952–2021) in a key hydrological recharge area of the eastern Iberian Peninsula. Atmos Res 286:1–19

Mishra AK, Singh VP (2010) A review of drought concepts. J Hydrol 391(1–2):204–216

Mlenga D, Jordaan A, Mandebvu B (2019) Monitoring droughts in Eswatini: a spatiotemporal variability analysis using the Standard Precipitation Index. Jàmbá J Disaster Risk Stud 11(1):1–11

Moreira E, Coelha C, Paulo A, Pereire L, Mexia J (2008) SPI-based drought category prediction using loglinear models. J Hydrol 354:116–130

Moriondo M, Giannakopoulos C, Bindi M (2011) Climate change impact assessment: the role of climate extremes in crop yield simulation. Clim Change (104):679–701

Ndayiragije J, Li F (2022) Effectiveness of drought indices in the assessment of different types of droughts, managing and mitigating their effects. Climate 10(125):1–21

Olgen KM (2010) Spatial distribution of annual and seasonal precipitation variability in Turkey. J Aegean Geogr 19(1):85–95

Olsen J, Dettinger M, Giovannettone J (2023) Drought attribution studies and water resources management. Bull Am Meteor Soc 104(2):E435–E441

Ozelkan E, Karaman M (2018) Analysis of the effect of meteorological and hydrological drought in Dam Lakes with multi-time satellite images: Atikhisar Dam (Çanakkale) example. Omer Halisdemir Univ J Eng Sci 7(2):1023–1037

Ozelkan E, Bagis S, Ozelkan C, Ustundag B, Yucel M, Ormeci C (2015) Spatial interpolation of climatic variables using land surface temperature and modified inverse distance weighting. Int J Remote Sens 36(4):1000–1025. https://doi.org/10.1080/01431161.2015.1007248

Ozelkan E, Chen G, Ustündag B (2016) Multiscale object-based drought monitoring and comparison in rainfed and irrigated agriculture from Landsat 8 OLI imagery. Int J Appl Earth Obs Geoinf 44:159–170

Palmer W (1965) Meteorologicak Drought. Research Paper No. 45; US Department of Commerce,Weather Bureau, Washington

Partal T, Yavuz E (2020) Application of trend analysis on drought indices in the Western Black Sea Region. Nat Disasters Appl Res Center J Nat Disasters Environ 6(2):345–353

Partigöc SN, Sogancı S (2019) The inevitable consequence of global climate change: drought. J Resilience 2(3):287–299

Pathak A, Dodamani B (2020) Comparison of meteorological drought indices for different climatic regions of an Indian River Basin. Asia Pac J Atmos Sci 56:563–576. https://doi.org/10.1007/s13143-019-00162-5

Pekpostalcı D, Tur R, Mehr A, Vazifekhah Ghaffari M, Dabrowska D, Nourani V (2023) Drought monitoring and forecasting across Turkey: a contemporary review. Sustainability 15(6080):1–23

Rousta I, Serif M, Heidari S, Kiani A, Ólafsson H, Kryszczak J, Baranowski P (2023) Climatic variables impact on inland lakes water levels and area fluctuations in an arid/semi-arid region of Iran, Iraq, and Turkey based on the remote sensing data. Earth Sci Inf 16(2):1611–1635

Sahana V, Mondal A (2023) Evolution of multivariate drought hazard, vulnerability and risk in India under climate change. Natural Hazards Earth Systm Sciences 23:623–641

Sahour H, Vazifedan M, Alshehri F (2020) Aridity trends in the Middle East and adjacent areas. Theoret Appl Climatol 142(3–4):1039–1054

Sen B, Topcu S, Türkes M, Sen B, Warner JF (2012) Projecting climate change, drought conditions and crops productivity in Turkey. Climate Res 52:175–191

Sensoy S, Demircan M, Ulupınar U, Balta I (2008) Climate of Turkey. State Meteorological Service (DMİ), Ankara

Simsek O, Cakmak B (2010) Drought Analysis for 2007–2008 Agricultural Year of Turkey. J Tekirdag Agric Fac 7(3):1–11

Simsek O, Yıldırım M, Gördebil N (2012) Drought Analysis of the 2011–2012 Agricultural Year. General Directorate of Meteorology, Research Department, Agricultural Meteorology Branch Directorate, Ankara

Simsek O, Yıldırım M, Gördebil N (2013) Drought analysis for the 2013–2014 agricultural year. General Directorate of Meteorology, Department of Research

Sobral B, Oliveira-Junior J, Gois G, Pereira-Junior E (2018) Spatial variability of SPI and RDIst drought indices applied to intense episodes of drought occurred in Rio de Janeiro State, Brazil. Int J Climat 38(10):3896–3916

Soľáková T, De Michele C, Vezzoli R (2013) Comparison between parametric and nonparametric approaches for the calculation of two drought indices: SPI and SSI. J Hydrol Eng 19(9):1–11

Stagge JH, Tallaksen LM, Gudmundsson L, Loonc AFV, Stahl K (2015) Candidate distributions for climatological drought indices (SPI and SPEI). Int J Climatol 35:4027–4040

Taskın O, Somuncu M, Capar G (2022) An assessment on the impacts of climate change on water resources and agriculture sector in Turkey. In: TUCAUM 2022 International Geography Symposium (Conference Paper). Ankara, pp 468–484

Tatlı H, Dalfes HN, Mentes SS (2004) A statistical downscaling method for monthly total precipitation over Turkey. International Jpurnal of Climatology 24:161–180

Tatlı H, Türkes M (2008) Determination of the link between the 2006/2007 drought in turkey and large-scale atmospheric variables by logistic regression. In: Proceedings of the IVth Atmospheric Sciences Symposium (Conference Paper), March 25–28, Istanbul, pp 516–527

Tigkas D, Vangelis H, Tsakiris G (2019) Drought characterisation based on an agriculture-oriented standardised precipitation index. Theoret Appl Climatol 135:1435–1447

Topcu E (2022) Appraisal of seasonal drought characteristics in Turkey during 1925–2016 with the standardized precipitation index and copula approach. Nat Hazards (112):697–723. https://doi.org/10.1007/s11069-021-05201-x

Tsakiris G, Vangelis H (2005) Establishing a drought index incorporating evapotranspiration. Eur Water 9(10):1–9

Tsakiris G, Pangalou D, Vangelis H (2007) Regional drought assessment based on the Reconnaissance Drought Index (RDI). Water Resource Manage 21:821–833

Tsakiris G (2004) Meteorological drought assessment. In: Paper prepared for the needs of the European Research Program MEDROPLAN (Conferance Paper) (Mediterranean Drought Preparedness and Mitigation Planning), Zaragoza, Spain

Türkes M (2007) Drought and desertification trend of Turkey and evaluation in respect to climate change. Pankobirlik 91:38–47

Türkes M (2012) Drought, desertification and a detailed analysis of the United Nations convention on combating desertification. Marmara Eur Stud Assoc 20(1):1–49

Türkes M (2020a) Climate and Drought in Turkey. In: Harmancıoğlu NB, Altinbilek D (eds) Water Resources of Turkey, World Water Resources. Springer, Vol. 2, pp 85–125

Türkes M (2020b) Impacts of climate change on agricultural production and food security: a scientific assessment. J Aegean Geogr 1(29):125–149

Türkes M, Erlat E (2003) Precipitation changes and variability in Turkey linked to the North Atlantic Oscillation during the period 1930–2000. Int J Climatol 23:1771–1796. https://doi.org/10.1002/joc.962

Türkeş M, Tatlı H (2009) Use of the standardized precipitation index (SPI) and a modified SPI for shaping the drought probabilities over Turkey. Int J Climatol 29:2270–2282. https://doi.org/10.1002/joc.1862

Varouchakis E (2021) Gaussian transformation methods for spatial data. Geosciences 11(196):1–9

Vicente-Serrano S, Begueria S, López-Moreno J (2010) Multiscalar drought index sensitive to global warming: the standardized precipitation evapotranspiration index. J Clim 23:1696–1718

Wang S, Huang HG, Lin GQ, Li Z, Zhang H, Fan RY (2014) Comparison of interpolation methods for estimating spatial distribution of precipitation in Ontario, Canada. Int J Climatol 34:3745–3751

Wilhite A, Glantz H (1985) Understanding the drought phenomenon: the role of definitions. Water Int 10(3):111–120

Willeke G, Hosking J, Wallis J, Guttman N (1994) The National Drought Atlas. Institute for Water Resources Report 94–NDS–4, U. S. Army Corps of Engineers, Washington

WMO (2012) Standardized precipitation index user guide. World Meteorological Organization. WMO-No. 1090

Xu K, Yang D, Yang H, Li Z, Qin Y, Shen Y (2015) Spatio-temporal variation of drought in China during 1961–2012: a climatic perspective. J Hydrol 526:253–264

Yang B, Cui Q, Meng Y, Zhang Z, Hong Z, Hu F, ... Zhang W (2023) Combined multivariate drought index for drought assessment in China from 2003 to 2020. Agric Water Manag 281. https://doi.org/10.1016/j.agwat.2023.108241

Yavuz H, Erdoğan S (2012) Spatial analysis of monthly and annual precipitation trends in Turkey. Water Resources Management: An International Journal, Published for the European Water Resources Association (EWRA), Springer; European Water Resources Association (EWRA) 26(3):609–621. https://doi.org/10.1007/s11269-011-9935-6

Yılmaz G (2023) Effects of drought and heat wave on agricultural production. J Nat Disasters Environ 9(2):240–257

Zarei A, Shabani A, Moghimi M (2021) Accuracy assessment of the SPEI, RDI and SPI drought indices in regions of Iran with different climate conditions. Pure Appl Geophys 178:1387–1403. https://doi.org/10.1007/s00024-021-02704-3

Zargar A, Sadiq R, Naser B, Khan F (2011) A review of drought indices. Environ Rev 19:333–349

Zeybekoglu U, Hezarani A, Keskin A (2023) Comparison of four precipitation based meteorological drought indices in the Yesilirmak Basin, Turkey. Q J Hung Meteorol Serv 127(1):123–142